

The gRAMP CRISPR-Cas effector is an RNA endonuclease complexed with a caspase-like peptidase

van Beljouw, S.P.B.; van Eijkeren-Haagsma, A.C.; Rodriguez Molina, A.; van den Berg, D.F.; Vink, J.N.A.; Brouns, S.J.J.

DOI

[10.1126/science.abk2718](https://doi.org/10.1126/science.abk2718)

Publication date

2021

Document Version

Accepted author manuscript

Published in

Science (New York, N.Y.)

Citation (APA)

van Beljouw, S. P. B., van Eijkeren-Haagsma, A. C., Rodriguez Molina, A., van den Berg, D. F., Vink, J. N. A., & Brouns, S. J. J. (2021). The gRAMP CRISPR-Cas effector is an RNA endonuclease complexed with a caspase-like peptidase. *Science (New York, N.Y.)*. <https://doi.org/10.1126/science.abk2718>

Important note

To cite this publication, please use the final published version (if applicable).
Please check the document version above.

Copyright

Other than for strictly personal use, it is not permitted to download, forward or distribute the text or part of it, without the consent of the author(s) and/or copyright holder(s), unless the work is under an open content license such as Creative Commons.

Takedown policy

Please contact us and provide details if you believe this document breaches copyrights.
We will remove access to the work immediately and investigate your claim.

Title: The gRAMP CRISPR-Cas effector is an RNA endonuclease complexed with a caspase-like peptidase

Authors: Sam P. B. van Beljouw^{1,2}, Anna C. Haagsma^{1,2}, Alicia Rodríguez-Molina^{1,2}, Daan F. van den Berg^{1,2}, Jochem N. A. Vink^{1,2}, Stan J. J. Brouns^{1,2*}

5 **Affiliations:**

¹Department of Bionanoscience, Delft University of Technology, Delft, Netherlands

²Kavli Institute of Nanoscience, Delft, Netherlands

*Corresponding author. Email: stanbrouns@gmail.com

10 **Abstract:** Type III CRISPR-Cas immunity is widespread in prokaryotes and is generally mediated by multi-subunit effector complexes. These complexes recognize complementary viral transcripts and can activate ancillary immune proteins. Here, we describe a type III-E effector from *Candidatus* “*Scalindua brodae*”, called *Sb*-gRAMP, which is natively encoded by a single gene with several type III domains fused together. This effector uses CRISPR RNA to guide target RNA
15 recognition and cleaves single-stranded RNA at two defined positions six nucleotides apart. Intriguingly, the *Sb*-gRAMP physically combines with the caspase-like TPR-CHAT peptidase to form the Craspase (CRISPR-guided Caspase) complex, pointing at a potential mechanism of target RNA-induced protease activity to gain viral immunity.

20 **One-Sentence Summary:** A single subunit type III-E effector cleaves RNA at two guide-defined positions and associates with a caspase-like peptidase.

Main Text: Facing constant predation by viruses and other mobile genetic elements (MGEs), prokaryotes have evolved multiple defense systems to protect themselves (1). Among those are the CRISPR-Cas systems, which provide adaptive immunity: invaders are recognized and inactivated by effector ribonucleoprotein complexes, during which genetic memory of the invader is generated and stored as spacers in CRISPR arrays (2). CRISPR-Cas effector complexes consist of CRISPR-associated (Cas) proteins bound to CRISPR RNA (crRNA) derived from a long transcript of the precursor CRISPR array (pre-crRNA) (3). Complementary binding of the crRNA to a target nucleic acid signifies the detection of an invader, setting the immune reaction in motion. Depending on the type of effector protein, immunity is typically reached either through direct cleavage of the invader's genetic material, or the activation of ancillary nucleases. CRISPR-Cas type III encompass both functionalities, making them among the most sophisticated CRISPR-Cas effector proteins known to date (4).

Recently, a new CRISPR-Cas subtype with resemblance to type III systems was bioinformatically predicted and classified as type III-E (5). Although type III-E effectors are related to other type III effectors (Fig. 1A), they are notably different in terms of protein architecture. Whereas type III effectors are typified by a multi-subunit composition, the type III-E effector seems to have various Repeat Associated Mysterious Protein (RAMP) domains fused together; hence the nickname g(iant)RAMP (5). The unusual size of approximately 1300 to 1900 amino acids makes gRAMP the largest single-unit effector found to date (Fig. 1B). We found that spacers embedded in type III-E CRISPR arrays have targets in MGEs (Fig. 1C; table S1) with a bias towards targeting the coding strand of open reading frames (Fig. 1D), indicating that gRAMP activity likely involves interaction with invader mRNA. Some type III-E loci carry Cas1 fused to a reverse transcriptase (fig. S1), suggesting that the type III-E acquisition machinery actively selects spacers from RNA (6). Curiously, the gRAMP gene clusters lack ancillary nuclease genes but often co-occur with a gene encoding a TPR-CHAT protein (fig. S1) (5), a caspase-like peptidase found to be involved in regulated bacterial cell death (7). This is suggestive of a functional relation between the CRISPR-Cas and caspase families in type III-E antiviral activity that we sought to uncover in the present study.

In order to investigate the molecular composition and function of the gRAMP protein, we selected gRAMP from the type III-E locus in *Candidatus* “*Scalindua brodae*” (*Sb*-gRAMP) (Fig. 1E) (8). We introduced an *Escherichia coli* codon optimized version of this protein into *E. coli*, together with a plasmid containing five copies of the first spacer from the native CRISPR array (Fig. 2A; table S2). We purified *Sb*-gRAMP to apparent homogeneity via three consecutive chromatography steps and observed distinct 260 nm absorption during size exclusion chromatography (SEC), indicative of co-purifying nucleic acids (fig. S2). Multi-angle light scattering (MALS) analysis indicated a homogenous particle of 242.5 ± 2.4 kDa (Fig. 2B), consistent with the expected size for a *Sb*-gRAMP monomer bound to an ssRNA species in the range of 45-60 nucleotides (nt) (Supplementary Text; table S3). Subsequent protein analysis showed a single band at the expected size for *Sb*-gRAMP (Fig. 2C). Nucleic acid extraction revealed the presence of three well-defined RNA populations of which the population at ~50 nt represents mature crRNA (Fig. 2D). These observations were reproducible when co-expressing *Sb*-gRAMP with a different repeat-spacer pair (fig. S3A-D), demonstrating that *Sb*-gRAMP can be loaded with a crRNA of choice.

The *Candidatus* “*Scalindua brodae*” type III-E locus contains a CRISPR array comprising 11 spacers interspaced by a 36 nt repeat sequence (table S2). To investigate the characteristics of mature crRNA in more detail, we PCR amplified the native CRISPR array from *Candidatus*

“*Scalindua brodae*” genomic DNA and co-expressed it with *Sb*-gRAMP. Following RNA extraction (fig. S4) and RNAseq (Fig. 2E; fig. S5), we determined that this RNA contains an unusually long 5'-handle of predominantly 27-28 nt, including the conserved last 14 nt of the repeat (Fig. 2F; fig. S6). Although a dominant spacer portion of 20 nt was observed, the vast majority of mature crRNAs were truncated within a window of 16-25 nt (Fig. 2F; fig. S3E; fig. S6B), suggestive of less specific processing on the 3'-end of the crRNA. In other type III systems, dedicated proteins (e.g. Cas6) are required for the generation of mature crRNA from pre-crRNA (9). Our discovery of spacer-sized RNA bound to *Sb*-gRAMP, combined with the absence of genes known to be involved in pre-crRNA processing (fig. S1) suggests that *Sb*-gRAMP might be capable of processing its own pre-crRNA, similar to Cas12 and Cas13 (10, 11). The larger RNA molecules bound by *Sb*-gRAMP might represent pre-crRNA processing intermediates. Notably, we obtained lower *Sb*-gRAMP protein yields and more degraded forms of *Sb*-gRAMP without the provision of pre-crRNA (Fig. 2G), suggesting an essential stabilizing or chaperoning role for the crRNA in *Sb*-gRAMP-crRNA complex formation. Hence, these results demonstrate that the *Sb*-gRAMP protein and a crRNA of typically 47 nt form a single ribonucleoprotein complex.

Given the apparent structural domain homology between *Sb*-gRAMP and subunits of other type III effectors, it seems plausible that *Sb*-gRAMP has evolved through a series of domain fusions and insertions. *Sb*-gRAMP contains a small domain with remote resemblance to Cas11 (Csm2) and four domains that possess structural homology to Cas7 (Csm3/Cmr4) subunits, one with a large insertion (Fig. 1E) (5). As Csm3/Cmr4 have been demonstrated to be responsible for target RNA cleavage in other type III systems (12, 13), we set out to investigate whether *Sb*-gRAMP also possesses endoribonuclease activity. We incubated purified *Sb*-gRAMP-crRNA with fluorescently labelled ssRNA substrates complementary to crRNA of spacer 1 (Fig. 3A) or spacer 3 (fig. S7A) and observed the appearance of two well-defined RNA cleavage products (Fig. 3B; fig. S7B), with the smaller product accumulating over time (fig. S8). Most target RNA remains uncleaved even at two-fold molar excess of gRAMP (fig. S9), suggesting that endoribonuclease activity only proceeds with a limited substrate turnover. Counting from the 5'-side of the crRNA into the target, the cleavage sites are located after nucleotides 3 (site 1) and 9 (site 2) relative to the crRNA, thus 6 nt apart (Fig. 3B; fig. S7C; fig. S10). When we tested target RNA substrates with the fluorescent label on the 3'-end instead of 5'-end, two smaller cleavage products accumulated with a 6 nt interval (Fig. 3B; fig. S11). This nucleotide spacing between cleavage sites is reminiscent of the 6 nt periodicity found for other type III effector complexes (14, 15), suggesting that the *Sb*-gRAMP retained the ancestral architectural positioning after domain fusion and insertion events. Also analogous to other type III effectors (16), complementarity between the protospacer flanking sequence (PFS) and the repeat portion of the crRNA retained the cleavage activity and positioning of *Sb*-gRAMP-crRNA within the complementary region of target RNA (Fig. 3C). Incubation of *Sb*-gRAMP-crRNA with an ssDNA target or non-complementary ssRNA substrate did not yield cleavage products (Fig. 3D). We also did not observe collateral RNase activity in the presence of a target RNA (fig. S12), demonstrating that *Sb*-gRAMP is a sequence and position specific crRNA-guided RNA endonuclease.

The CRISPR-Cas type III Csm3/Cmr4 domains harbor acidic residues essential for metal-ion coordination and subsequent ribonuclease catalysis (14, 15, 17). The removal of divalent cations from the cleavage buffer abolished *Sb*-gRAMP-crRNA ability to cleave target RNA (Fig. 3E), showing that RNase activity was dependent on metal ions. This raised the possibility that *Sb*-gRAMP possesses acidic amino acid residues essential for a functional endoribonuclease active site, akin to ancestral Csm3/Cmr4. To test this, we identified seven conserved aspartic acids and

one serine residue that might be active in the ribonuclease catalytic core, based on multiple sequence alignment of various gRAMPs (fig. S13) and structural similarity to the *Streptococcus thermophilus* Csm3 structure (12) (fig. S14). Mutational analysis of these positions indeed revealed that *Sb*-gRAMP-crRNA lost its target RNA cleavage ability at site 2 upon changing a single aspartic acid residue to an alanine (D698A) (Fig. 3F). The single amino acid change renders a *Sb*-gRAMP variant able to sequence specifically cleave target RNA only at site 1, which may provide distinct benefits for biotechnological application where specific single RNA cleavage is desired. Despite trying the eight positions (fig. S15), the low sequence similarity of gRAMPs to Csm3/Cmr4 did not permit identifying essential active site residues responsible for the cleavage at site 1 and may require structural analysis. Currently described type III effectors cleave RNA once per Csm3/Cmr4 subunit; *Sb*-gRAMP, composed of four Csm3-like domains, only cleaves twice under our experimental conditions (Fig. 3G). This suggests that the other ribonuclease domains were either rendered dysfunctional over time or evolved into other functionalities.

In canonical type III systems, RNA target recognition with mismatching PFS leads to the activation of the cyclase domain in the Cas10 subunit, which in turn synthesizes cyclic oligo adenylates (cOAs) (18, 19). The cOAs act as allosteric activators of ancillary proteins often found in or near the CRISPR-Cas loci by binding in the CRISPR-associated Rossmann Fold (CARF) domain (20). It appears that the Cas10 subunit as well as CARF-containing proteins were lost during the evolutionary genesis of gRAMP (5). Since this makes cOA signaling in type III-E unlikely, we wondered what the functional relation could be with the co-occurring caspase-like protease TPR-CHAT (fig. S1) (5). The tetratricopeptide repeat (TPR) domain is often involved in protein-protein interaction and the formation of protein complexes (21), which prompted us to test physical association between TPR-CHAT and *Sb*-gRAMP-crRNA.

To assess potential interaction, we affinity purified either *Sb*-gRAMP-crRNA or TPR-CHAT from cells that co-expressed both proteins (Fig. 4A) and observed co-elution using either protein as a bait (Fig. 4B; fig. S16A). This indicated the formation of a stable complex between *Sb*-gRAMP-crRNA and TPR-CHAT (table S4), whose interaction was retained during subsequent heparin chromatography and SEC (Fig. 4B; fig. S17). MALS revealed a single, homogenous population with a molar mass of 315.4 ± 2.8 kDa (Fig. 4C; fig. S18), corresponding to *Sb*-gRAMP-crRNA and TPR-CHAT complexed in a 1:1 stoichiometry (table S3). The retention time of the complex was shorter than that of *Sb*-gRAMP-crRNA alone, consistent with a particle of higher molecular weight (fig. S19). The heparin purified complex contained mature crRNA (Fig. 4D) with 6 nt spaced cleavage specificity towards target RNA (Fig. 4E; fig. S20; fig. S16B). TPR-CHAT with inactivated predicted catalytic residues (H585A and C627A) (7) was also able to associate with *Sb*-gRAMP-crRNA (fig. S16), indicating that complex formation occurs independently of TPR-CHAT activity. TPR-CHAT did not dissociate from *Sb*-gRAMP-crRNA in the presence of target RNA (fig. S21), suggesting that *Sb*-gRAMP-crRNA and TPR-CHAT form a stable protein complex which remains assembled upon target RNA recognition. We here name this complex Craspase (CRISPR-guided Caspase).

The TPR-CHAT is a predicted protease from the caspase family whose members typically catalyze the hydrolysis of specific peptide bonds of target proteins (22), many of which remain to be identified. Pathways involving caspase-like proteins are often activated during eukaryotic apoptosis, but are also abundant in the bacterial kingdom where they have been shown to function in regulated cell death (7). To test whether we could trigger cell death with the Craspase complex, we co-expressed it with an inducible target RNA in *E. coli* and followed the growth kinetics of the

bacteria. We did not observe growth defects upon target RNA production (fig. S22), suggesting the absence of the target protein in the transplanted *E. coli* host, the requirement of additional factors for Craspase activation, or a biological role for Craspase in a context other than cell-death induction.

5 The type III-E gRAMP effector has characteristics of both CRISPR-Cas Class 1 (e.g. type III domains, six nucleotide cleavage spacing, cleavage of RNA independent of matching PFS) and Class 2 (e.g. single protein composition), blurring the boundaries of the traditional CRISPR-Cas classification. Its physical association with TPR-CHAT raises the possibility of crRNA-guided caspase-like activity to reach viral immunity. Although the specific RNA cleavage capability of
10 gRAMP-crRNA could contribute to direct antiviral defense, the primary role of target RNA recognition and cleavage may instead be the on and off switching of Craspase. This switching has been observed in other type III systems, where RNA target interaction regulates second messenger production which in turn controls ancillary nuclease activity (23, 24). Our findings that *Sb*-gRAMP-crRNA targets RNA and forms a stable complex with TPR-CHAT give rise to a model
15 in which gRAMP-crRNA, instead of using second messengers, allosterically induces peptidase activity upon target RNA recognition to elicit a specific immune response (Fig. 4F).

References and Notes

1. S. Doron, S. Melamed, G. Ofir, A. Leavitt, A. Lopatina, M. Keren, G. Amitai, R. Sorek, Systematic discovery of antiphage defense systems in the microbial pangenome. *Science*. **359**, eaar4120 (2018).
2. R. Barrangou, C. Fremaux, H. Deveau, M. Richardss, P. Boyaval, S. Moineau, D. A. Romero, P. Horvath, CRISPR Provides Acquired Resistance Against Viruses in Prokaryotes. *Science*. **315**, 1709–1712 (2007).
3. S. J. J. Brouns, M. M. Jore, M. Lundgren, E. R. Westra, R. J. H. Slijkhuis, A. P. L. Snijders, M. J. Dickman, K. S. Makarova, E. V. Koonin, J. Van Der Oost, Small CRISPR RNAs guide antiviral defense in prokaryotes. *Science*. **321**, 960–964 (2008).
4. R. Molina, N. Sofos, G. Montoya, Structural basis of CRISPR-Cas Type III prokaryotic defence systems. *Curr. Opin. Struct. Biol.* **65**, 119–129 (2020).
5. K. S. Makarova, Y. I. Wolf, J. Iranzo, S. A. Shmakov, O. S. Alkhnbashi, S. J. J. Brouns, E. Charpentier, D. Cheng, D. H. Haft, P. Horvath, S. Moineau, F. J. M. Mojica, D. Scott, S. A. Shah, V. Siksnys, M. P. Terns, Č. Venclovas, M. F. White, A. F. Yakunin, W. Yan, F. Zhang, R. A. Garrett, R. Backofen, J. van der Oost, R. Barrangou, E. V. Koonin, Evolutionary classification of CRISPR–Cas systems: a burst of class 2 and derived variants. *Nat. Rev. Microbiol.* **18**, 67–83 (2020).
6. S. Silas, G. Mohr, D. J. Sidote, L. M. Markham, A. Sanchez-Amat, D. Bhaya, A. M. Lambowitz, A. Z. Fire, Direct CRISPR spacer acquisition from RNA by a natural reverse transcriptase-Cas1 fusion protein. *Science*. **351**, aad4234 (2016).
7. A. G. Johnson, T. Wein, M. L. Mayer, B. Duncan-lowey, E. Yirmiya, Bacterial gasdermins reveal an ancient mechanism of cell death. *bioRxiv*, 1–36 (2021).
8. M. Schmid, K. Walsh, R. Webb, W. I. C. Rijpstra, K. Van De Pas-Schoonen, M. J. Verbruggen, T. Hill, B. Moffett, J. Fuerst, S. Schouten, J. S. S. Damsté, J. Harris, P. Shaw, M. Jetten, M. Strous, Candidatus “*Scalindua brodae*”, sp. nov., Candidatus “*Scalindua wagneri*”, sp. nov., Two New Species of Anaerobic Ammonium Oxidizing Bacteria. *Syst. Appl. Microbiol.* **26**, 529–538 (2003).
9. F. C. Walker, L. Chou-Zheng, J. A. Dunkle, A. Hatoum-Aslan, Molecular determinants for CRISPR RNA maturation in the Cas10-Csm complex and roles for non-Cas nucleases. *Nucleic Acids Res.* **45**, 2112–2123 (2017).
10. I. Fonfara, H. Richter, M. Bratoviä, A. Le Rhun, E. Charpentier, The CRISPR-associated DNA-cleaving enzyme Cpf1 also processes precursor CRISPR RNA. *Nature*. **532**, 517–521 (2016).
11. A. East-Seletsky, M. R. O’Connell, S. C. Knight, D. Burstein, J. H. D. Cate, R. Tjian, J. A. Doudna, Two distinct RNase activities of CRISPR-C2c2 enable guide-RNA processing and RNA detection. *Nature*. **538**, 270–273 (2016).
12. L. You, J. Ma, J. Wang, D. Artamonova, M. Wang, L. Liu, H. Xiang, K. Severinov, X. Zhang, Y. Wang, Structure Studies of the CRISPR-Csm Complex Reveal Mechanism of Co-transcriptional Interference. *Cell*. **176**, 239–253 (2019).
13. C. Benda, J. Ebert, R. A. Scheltema, H. B. Schiller, M. Baumgärtner, F. Bonneau, M. Mann, E. Conti, Structural model of a CRISPR RNA-silencing complex reveals the RNA-target cleavage activity in Cmr4. *Mol. Cell*. **56**, 43–54 (2014).
14. R. H. J. Staals, Y. Zhu, D. W. Taylor, J. E. Kornfeld, K. Sharma, A. Barendregt, J. J. Koehorst, M. Vlot, N. Neupane, K. Varossieau, K. Sakamoto, T. Suzuki, N. Dohmae, S. Yokoyama, P. J. Schaap, H. Urlaub, A. J. R. Heck, E. Nogales, J. A. Doudna, A. Shinkai, J. van der Oost, RNA Targeting by the Type III-A CRISPR-Cas Csm Complex of *Thermus thermophilus*. *Mol. Cell*. **56**, 518–530 (2014).
15. G. Tamulaitis, M. Kazlauskienė, E. Manakova, Č. Venclovas, A. O. Nwokeoji, M. J. Dickman, P. Horvath, V. Siksnys, Programmable RNA Shredding by the Type III-A CRISPR-Cas System of *Streptococcus thermophilus*. *Mol. Cell*. **56**, 506–517 (2014).
16. M. P. Terns, CRISPR-Based Technologies: Impact of RNA-Targeting Systems. *Mol. Cell*. **72**, 404–412 (2018).
17. C. R. Hale, P. Zhao, S. Olson, M. O. Duff, B. R. Graveley, L. Wells, R. M. Terns, M. P. Terns, RNA-Guided RNA Cleavage by a CRISPR RNA-Cas Protein Complex. *Cell*. **139**, 945–956 (2009).
18. M. Kazlauskienė, G. Kostiuik, Č. Venclovas, G. Tamulaitis, V. Siksnys, A cyclic oligonucleotide signaling pathway in type III CRISPR-Cas systems. *Science*. **357**, 605–609 (2017).
19. O. Niewoehner, C. Garcia-Doval, J. T. Rostøl, C. Berk, F. Schwede, L. Bigler, J. Hall, L. A. Marraffini, M. Jinek, Type III CRISPR-Cas systems produce cyclic oligoadenylate second messengers. *Nature*. **548**, 543–548 (2017).
20. K. S. Makarova, V. Anantharaman, N. V. Grishin, E. V. Koonin, L. Aravind, CARF and WYL domains: Ligand-binding regulators of prokaryotic defense systems. *Front. Genet.* **5**, 102 (2014).

21. L. D. D'Andrea, L. Regan, TPR proteins: The versatile helix. *Trends Biochem. Sci.* **28**, 655–662 (2003).
22. L. Aravind, E. V. Koonin, Classification of the caspase-hemoglobinase fold: Detection of new families and implications for the origin of the eukaryotic separins. *Proteins Struct. Funct. Genet.* **46**, 355–367 (2002).
23. C. Rouillon, J. S. Athukoralage, S. Graham, S. Grischow, M. F. White, Control of cyclic oligoadenylate synthesis in a type III CRISPR system. *Elife*. **7**, 1–22 (2018).
24. J. A. Steens, Y. Zhu, D. W. Taylor, J. P. K. Bravo, S. H. . Prinsen, C. D. Schoen, B. J. . Keijser, M. Ossendrijver, L. M. Hofstra, S. J. J. Brouns, A. Shinkai, J. van der Oost, R. H. J. Staals, SCOPE: Flexible targeting and stringent CARF activation enables type III CRISPR-Cas diagnostics. *bioRxiv*, 1–27 (2021).
25. P. Pausch, B. Al-Shayeb, E. Bisom-Rapp, C. A. Tsuchida, Z. Li, B. F. Cress, G. J. Knott, S. E. Jacobsen, J. F. Banfield, J. A. Doudna, Crispr-casΦ from huge phages is a hypercompact genome editor. *Science*. **369**, 333–337 (2020).
26. M. Martin, Cutadapt Removes Adapter Sequences From High-Throughput Sequencing Reads. *EMBnet. J.* **17**, 10–12 (2011).
27. H. Li, Minimap2: Pairwise alignment for nucleotide sequences. *Bioinformatics*. **34**, 3094–3100 (2018).
28. E. Gasteiger, C. Hoogland, A. Gattiker, M. R. Wilkins, R. D. Appel, A. Bairoch, Protein identification and analysis tools on the ExPASy server. *proteomics Protoc. Handb.*, 571–607 (2005).
29. M. Pabst, D. Grouzdev, C. E. Lawson, H. B. C. Kleikamp, C. de Ram, R. Louwen, Y. Lin, S. Lücker, M. C. M. van Loosdrecht, M. Laureni, A general approach to explore prokaryotic protein glycosylation reveals the unique surface layer modulation of an anammox bacterium. *bioRxiv*, 1–18 (2020).
30. M. Steinegger, J. Söding, MMseqs2 enables sensitive protein sequence searching for the analysis of massive data sets. *Nat. Biotechnol.* **35**, 1026–1028 (2017).
31. J. Söding, A. Biegert, A. N. Lupas, The HHpred interactive server for protein homology detection and structure prediction. *Nucleic Acids Res.* **33**, 244–248 (2005).
32. J. Russel, R. Pinilla-Redondo, D. Mayo-Muñoz, S. A. Shah, S. J. Sørensen, CRISPRCasTyper: Automated Identification, Annotation, and Classification of CRISPR-Cas Loci. *Cris. J.* **3**, 462–469 (2020).
33. J. N. A. Vink, J. H. L. Baijens, S. J. J. Brouns, Comprehensive PAM prediction for CRISPR-Cas systems reveals evidence for spacer sharing, preferred strand targeting and conserved links with CRISPR repeats. *bioRxiv*, 1–42 (2021).
34. T. Seemann, Prokka: Rapid prokaryotic genome annotation. *Bioinformatics*. **30**, 2068–2069 (2014).
35. L. J. H. Doug Hyatt, Gwo-Liang Chen, Philip F LoCascio, Miriam L Land, , Frank W Larimer, Prodigal: prokaryotic gene recognition and translation initiation site identification. *BMC Bioinformatics*. **11** (2010).
36. L. Fu, B. Niu, Z. Zhu, S. Wu, W. Li, CD-HIT: Accelerated for clustering the next-generation sequencing data. *Bioinformatics*. **28**, 3150–3152 (2012).
37. K. Katoh, H. Toh, Parallelization of the MAFFT multiple sequence alignment program. *Bioinformatics*. **26**, 1899–1900 (2010).
38. S. Capella-Gutiérrez, J. M. Silla-Martínez, T. Gabaldón, trimAl: A tool for automated alignment trimming in large-scale phylogenetic analyses. *Bioinformatics*. **25**, 1972–1973 (2009).
39. L. T. Nguyen, H. A. Schmidt, A. Von Haeseler, B. Q. Minh, IQ-TREE: A fast and effective stochastic algorithm for estimating maximum-likelihood phylogenies. *Mol. Biol. Evol.* **32**, 268–274 (2015).
40. I. Letunic, P. Bork, Interactive Tree of Life (iTOL) v4: Recent updates and new developments. *Nucleic Acids Res.* **47**, 256–259 (2019).
41. J. S. Papadopoulos, R. Agarwala, COBALT: Constraint-based alignment tool for multiple protein sequences. *Bioinformatics*. **23**, 1073–1079 (2007).
42. A. M. Waterhouse, J. B. Procter, D. M. A. Martin, M. Clamp, G. J. Barton, Jalview Version 2-A multiple sequence alignment editor and analysis workbench. *Bioinformatics*. **25**, 1189–1191 (2009).
43. X. Robert, P. Gouet, Deciphering key features in protein structures with the new ENDScript server. *Nucleic Acids Res.* **42**, 320–324 (2014).
44. L. A. Kelley, S. Mezulis, C. M. Yates, M. N. Wass, M. J. E. Sternberg, The Phyre2 web portal for protein modeling, prediction and analysis. *Nat. Protoc.* **10**, 845–858 (2015).
45. W. L. DeLano, Pymol: An open-source molecular graphics tool. *CCP4 Newsl. protein Crystallogr.* **40**, 82–92 (2002).

Acknowledgements: We kindly thank Dr. Mike Jetten and Guylaine Nuijten (Radboud University) for the provision of *Candidatus* “*Scalindua brodae*” gDNA, Dr. Cecilia de Agrela Pinto (Delft University of Technology) for performing SEC-MALS analysis, Dr. Martin Pabst and Carol de Ram (Delft University of Technology) for performing mass spectrometry analysis, and Dr. Robert Mans, Charlotte Koster, Carolien Bastiaanssen and Jaco van der Torre (Delft University of Technology) for provision of equipment and reagents. We thank Brouns Lab members for helpful discussions, and Dr. Ana Rita Costa (Delft University of Technology) for experimental help during revisions.

Funding:

SJJB is supported by the Netherlands Organisation for Scientific Research (NWO VICI; VI.C.182.027) and has received funding from the European Research Council (ERC) CoG under the European Union’s Horizon 2020 research and innovation programme (grant agreement No. [101003229]).

Author contributions:

Conceptualization: SPBB, SJJB

Experimental work: SPBB, ACH, ARM

Bioinformatics analysis: SPBB, DFB, JNAV

Funding acquisition: SJJB

Writing – original draft: SPBB, SJJB

Writing – review & editing: SPBB, SJJB, with input from all other authors

Competing interests: SPBB and SJJB are inventors on patent application N2028346 submitted by Delft University of Technology that covers uses of gRAMP and Craspase.

Data and materials availability: All data are available in the manuscript or the supplementary material. Plasmids and strains are available upon request from SJJB.

Supplementary Materials

Materials and Methods

Supplementary Text

Figs. S1 to S22

Tables S1 to S8

References (26-45)

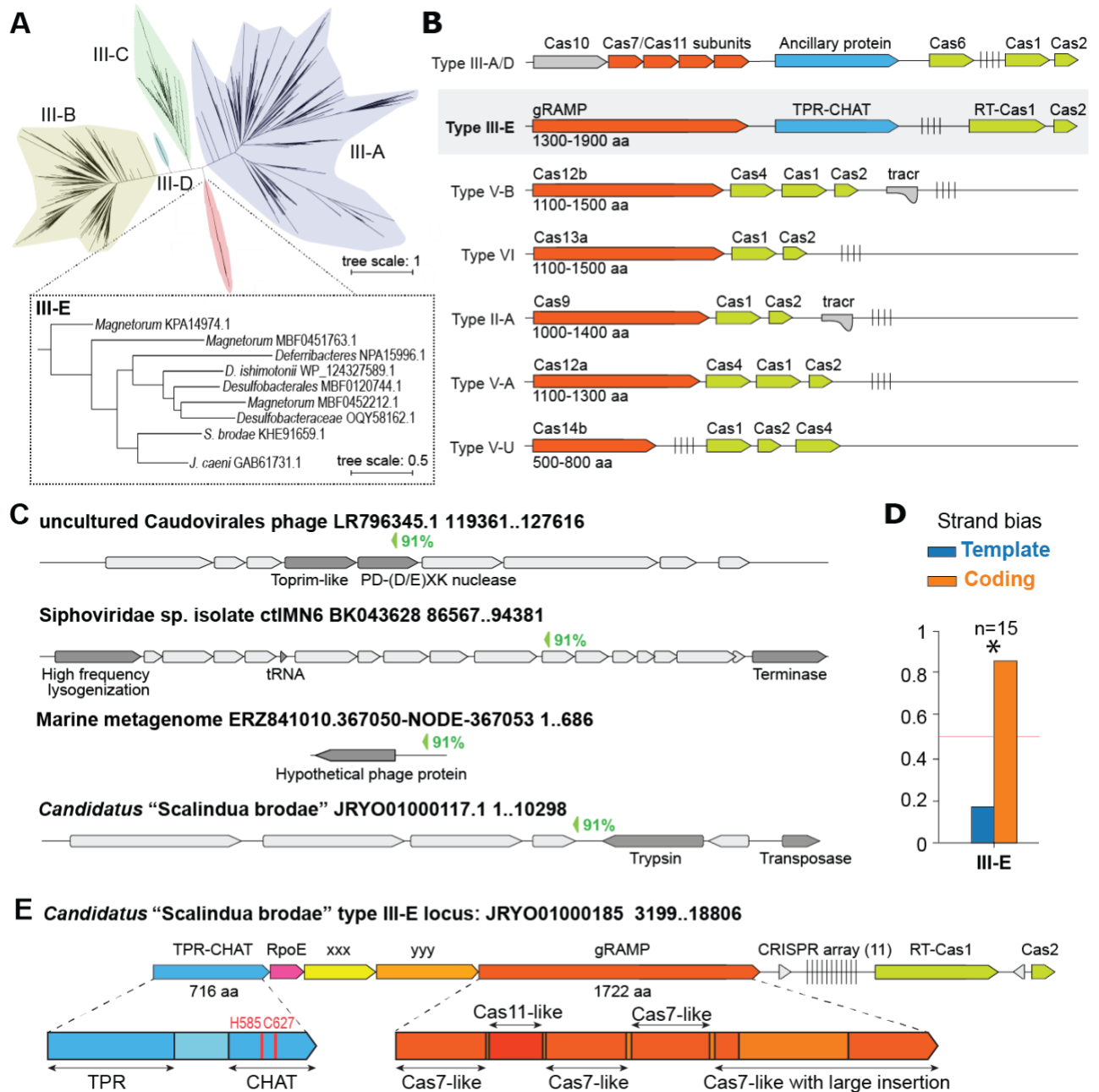


Fig. 1. CRISPR-Cas type III-E composition and characteristics. (A) Phylogenetic tree of type III subunit proteins (Csm3 and Cmr4) compiled with type III-E gRAMPs. The tree scale bar represents the number of substitutions per site. (B) Illustrations of typical organization of CRISPR-Cas types with sizes of effector proteins indicated in the number of amino acids (25). (C) Examples of contigs with matches to spacers from type III-E CRISPR arrays. (D) Fraction of spacers found in type III-E CRISPR arrays targeting template or coding strand ($p = 0.011$). (E) Detailed outline of the type III-E locus from *Candidatus* "Scalindua brodae".

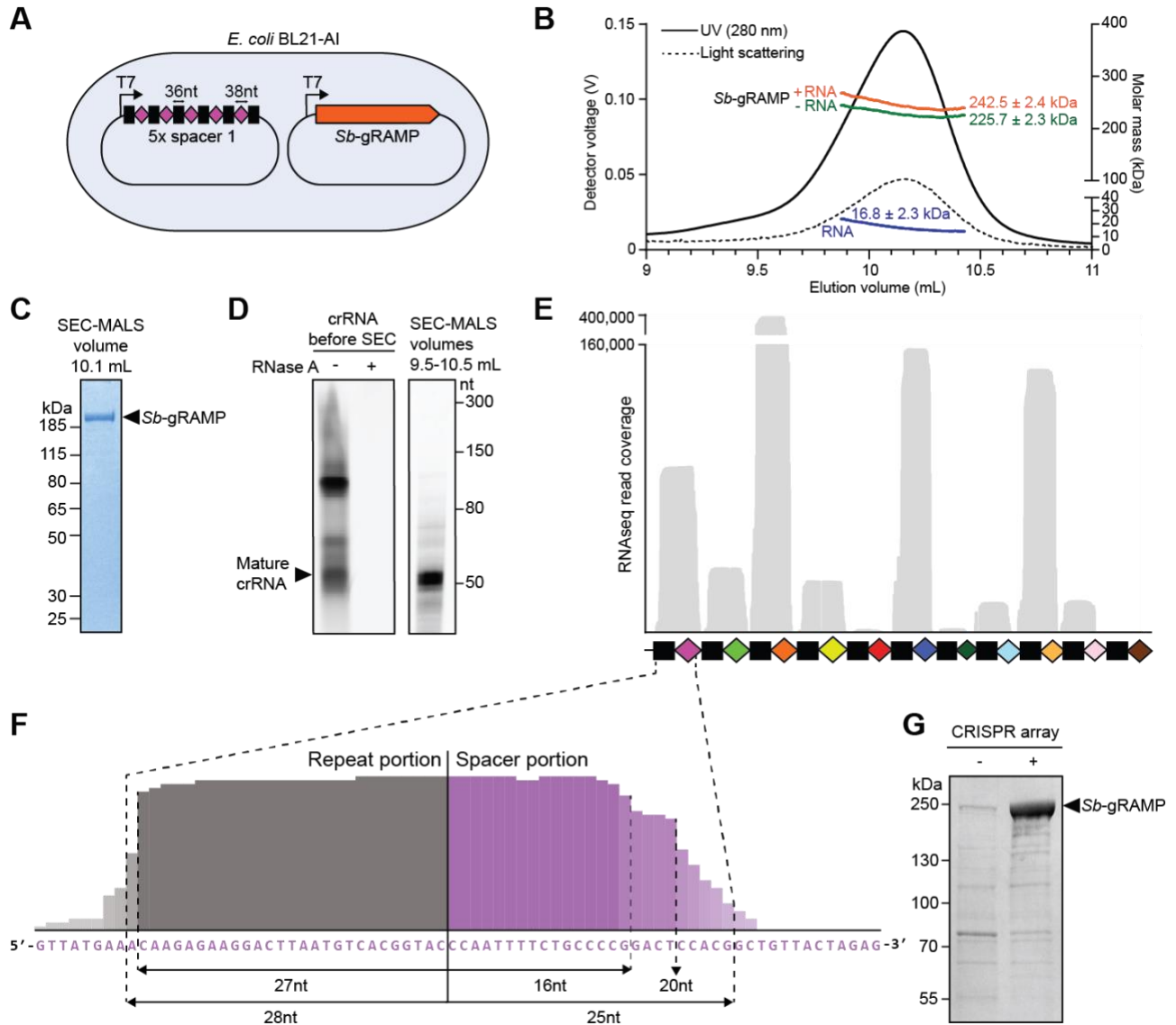


Fig. 2. *Sb-gRAMP-crRNA* is a ribonucleoprotein encoded by a single open reading frame. (A) Schematic of the heterologous expression system used for *Sb-gRAMP-crRNA1* overexpression. (B) SEC-MALS peaks corresponding to light scattering and UV₂₈₀ absorbance profiles of purified *Sb-gRAMP-crRNA1*. The molar masses are derived from the peak half-height region (9.9-10.4 mL). (C) SDS-PAGE analysis after SEC-MALS. (D) Denaturing urea PAGE analysis of the nucleic acid content in *Sb-gRAMP-crRNA1*. (E) RNA sequencing reads of native crRNA with length 40 to 60 nucleotides mapped onto the native CRISPR array. (F) RNaseq read depth of the first repeat-spacer with predominant repeat and spacer lengths indicated based on consensus processing. (G) SDS-PAGE analysis of *Sb-gRAMP* protein expressed in the absence and presence of a CRISPR array with five copies of spacer 1.

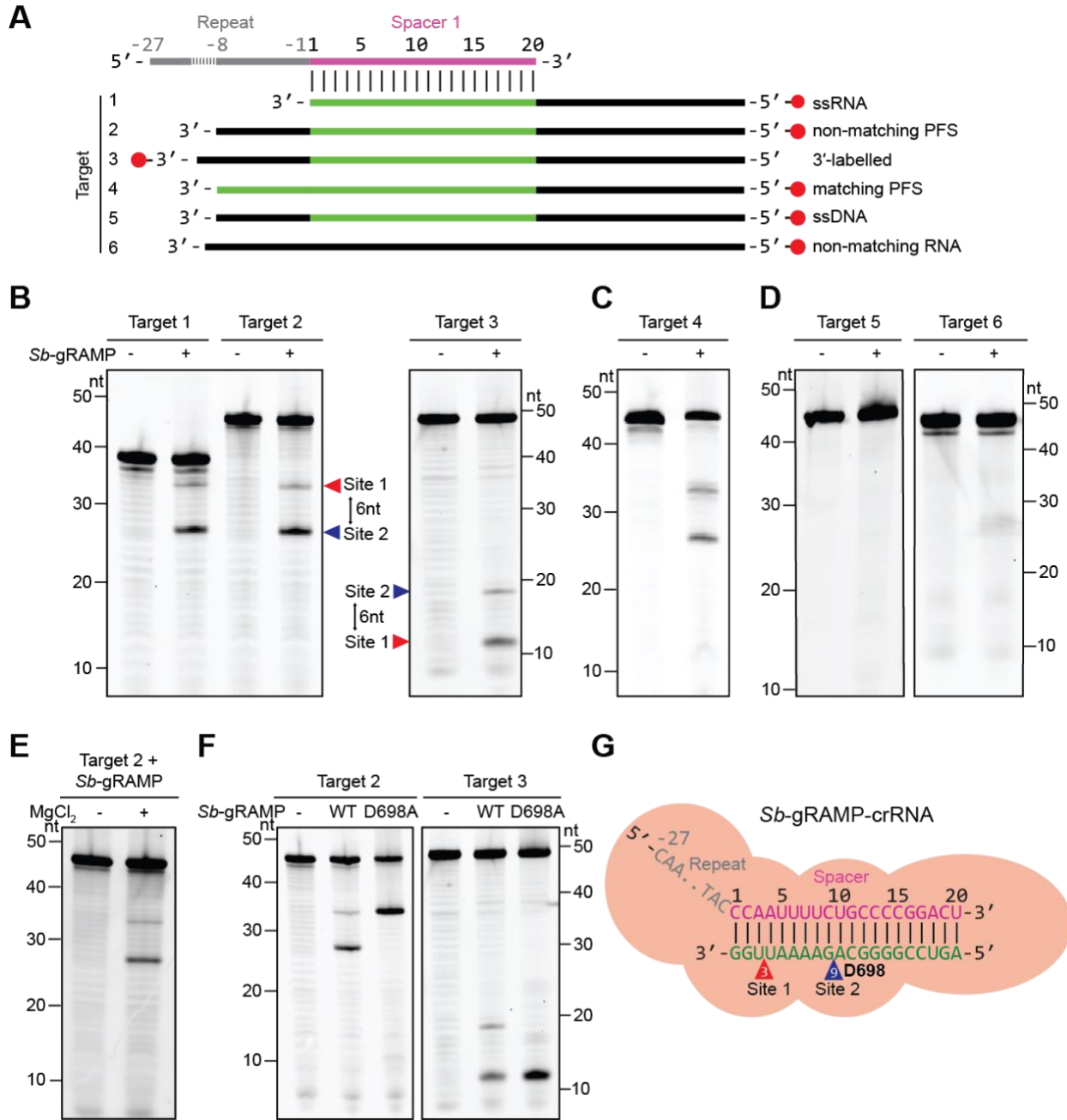


Fig. 3. *Sb-gRAMP*-crRNA drives dual ssRNA cleavage with six nt spacing. (A) Outline of the Cy5-labelled nucleic acid targets tested for *Sb-gRAMP*-crRNA1 activity. (B-F) Denaturing urea PAGE gels of *Sb-gRAMP*-crRNA1 incubated with (B) complementary ssRNA (cleavage products indicated with arrowheads), (C) ssRNA with a matching PFS, (D) complementary ssDNA and non-complementary ssRNA, (E) complementary ssRNA in the presence or absence of MgCl₂ and (F) with *Sb-gRAMP*-crRNA1 containing the D698A inactivating mutation. (G) Schematic of *Sb-gRAMP*-crRNA1 hybridized to an ssRNA target with the exact cleavage sites indicated.

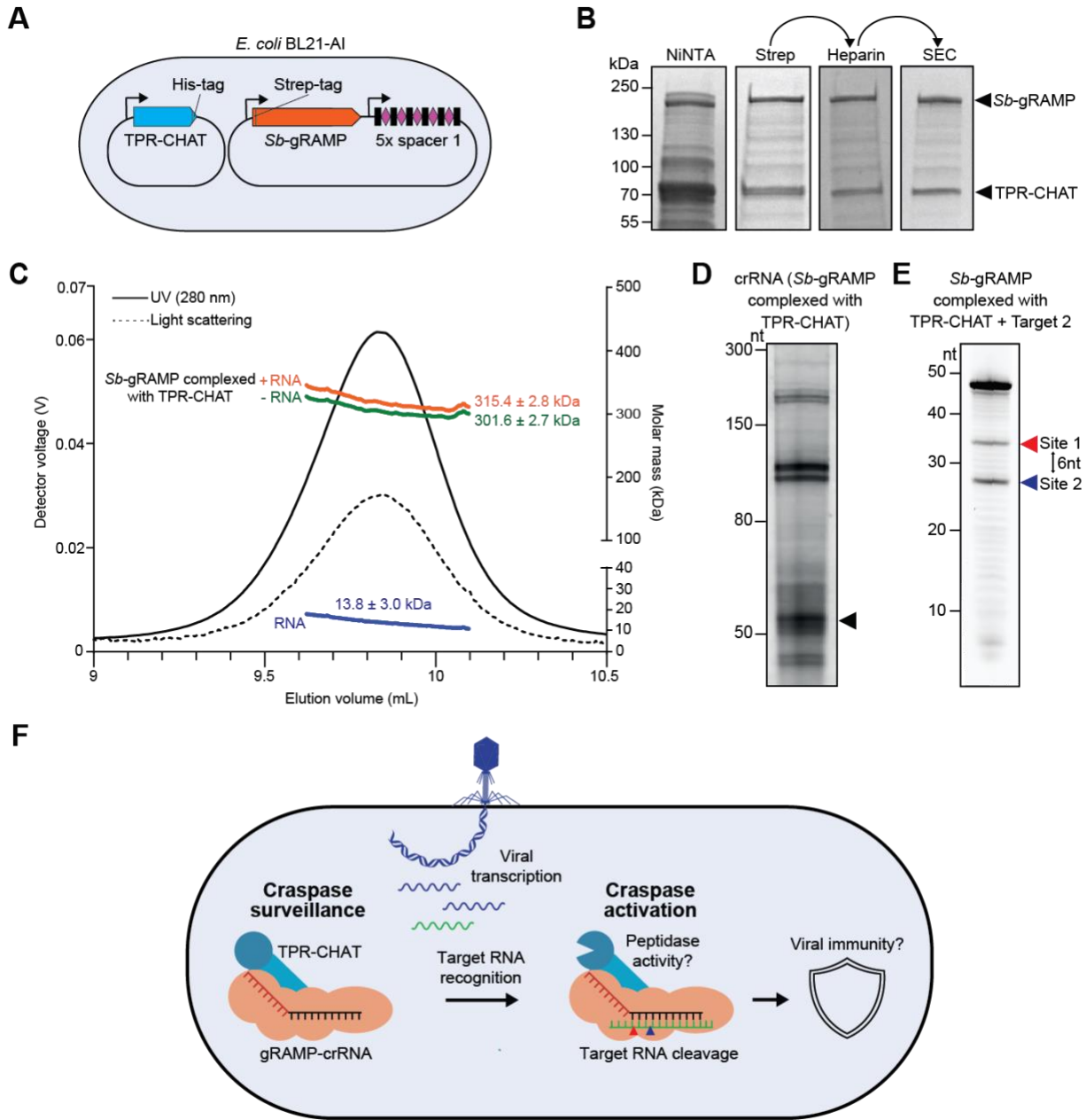


Fig. 4. *Sb*-gRAMP-crRNA and TPR-CHAT form the stable Craspase complex. (A) Schematic of the expression system used for overexpression of TPR-CHAT and *Sb*-gRAMP-crRNA1. (B) SDS-PAGE gels after the subsequent purification steps of *Sb*-gRAMP-crRNA1 complexed with TPR-CHAT. (C) SEC-MALS light scattering UV₂₈₀ absorbance profiles of *Sb*-gRAMP-crRNA1 complexed with TPR-CHAT. Molar masses are derived from the peak half-height region (9.6-10.1 mL). (D) Denaturing urea PAGE gel of RNA extracted from heparin purified *Sb*-gRAMP-crRNA1 complexed with TPR-CHAT. Mature crRNA size is indicated with a black arrowhead and is based on the mature crRNA fraction found in *Sb*-gRAMP-crRNA1. (E) Denaturing urea PAGE gel of target cleavage by heparin purified *Sb*-gRAMP-crRNA1 complexed with TPR-CHAT. Cleavage products are indicated with arrowheads. (F) Model of CRISPR-Cas type III-E during phage infection.

Supplementary Materials for

5 **Title: The gRAMP CRISPR-Cas effector is an RNA endonuclease complexed with a caspase-like peptidase**

Authors: Sam P. B. van Beljouw^{1,2}, Anna C. Haagsma^{1,2}, Alicia Rodríguez-Molina^{1,2}, Daan F. van den Berg^{1,2}, Jochem N. A. Vink^{1,2}, Stan J. J. Brouns^{1,2*}

Correspondence to: stanbrouns@gmail.com

10

This PDF file includes:

Materials and Methods

Supplementary Text

15

Figs. S1 to S22

Tables S1 to S8

Materials and Methods

Plasmid cloning

Plasmids used in this study are listed in table S6. Primers described in table S7 were used for PCR amplification using the Q5 high-fidelity Polymerase (New England Biolabs). Ordered DNA sequences are listed in table S8. All plasmids were verified by Sanger-sequencing (Macrogen Europe, Amsterdam, The Netherlands). Cloning was performed using NEBuilder HiFi DNA Assembly (New England Biolabs) unless stated otherwise. Bacterial transformations for cloning were performed using NEB® 5-alpha Competent *E. coli* (New England Biolabs) and carried out by electroporation using ECM630 Electrocell Manipulator (2.5 kV, 200 Ω , 25 μ F).

For the expression of *Candidatus* “*Scalindua brodae*” gRAMP (*Sb*-gRAMP), a two-plasmid expression system was used: a plasmid containing the gRAMP protein (pGRAMP) and a plasmid containing the CRISPR RNA (pCRISPR-1, pCRISPR-3 or pCRISPR-WT). To construct pGRAMP, a coding sequence corresponding to an *E. coli* codon-optimized gRAMP protein variant containing a N-terminal Twin-Strep-Tag II and a SUMO-tag was designed, ordered (Life Technologies Europe BV) and cloned downstream of the LacI repressed T7 promoter on the plasmid 13S-S (encoding spectinomycin resistance for selection) (Berkeley MacroLab). pGRAMP variants with mutations were generated by amplifying pGRAMP with primers containing the desired mutations.

To construct pCRISPR-1 and pCRISPR-3, a CRISPR array starting with the native *Candidatus* “*Scalindua brodae*” leader sequence, followed by six native repeats interspaced by five times the first spacer (pCRISPR-1) or the third spacer (pCRISPR-3) in the native CRISPR array was designed, ordered (Life Technologies Europe BV) and cloned downstream of the LacI repressed T7 promoter on pACYC Duet-1 (encoding chloramphenicol resistance for selection) (Novagen EMD Millipore) by restriction with MfeI-HF (New England Biolabs) and NdeI (New England Biolabs) followed by ligation with T4 DNA ligase (New England Biolabs). To construct pCRISPR-WT, the native type III-E CRISPR array was PCR amplified from *Candidatus* “*Scalindua brodae*” genomic DNA and cloned downstream of the LacI repressed T7 promoter on pACYC Duet-1. In order to get both the *Sb*-gRAMP protein and the CRISPR-1 array encoded on the same plasmid, the CRISPR array was PCR amplified from pCRISPR-1 and assembled with PCR amplified pGRAMP to yield pGRAMP-CRISPR-1. For the co-expression of an RNA target cognate to crRNA-1, a plasmid (pTarget) encoding the complementary target DNA (5' -

CTCTAGTAACAGCCGTGGAGTCCGGGGCAGAAAATTGG - 3') downstream of the LacI repressed T7 promoter was generated via “around-the-horn” PCR amplification and self-ligation of p13S-S using phosphorylated primers with flags encoding the target sequence. The region including the LacI repressed T7 promoter, DNA encoding the RNA target cognate to crRNA-1 and downstream T7 terminator was subsequently PCR amplified from pTarget and integrated in pGRAMP-CRISPR-1 to yield pGRAMP-CRISPR-1-target-1.

For the expression of *Candidatus* “Scalindua brodae” TPR-CHAT, a coding sequence corresponding to an *E. coli* codon-optimized TPR-CHAT protein variant containing a C-terminal His-tag was designed and ordered as a gBlock (Integrated DNA Technologies) and cloned downstream of the LacI repressed T7 promoter on the plasmid pACYC Duet-1 to yield pTPR-CHAT. pTPR-CHAT H585A C627A was constructed via insertion of a gBlock containing the desired mutations into pTPR-CHAT.

Protein overexpression for purification

Electrocompetent cells *E. coli* BL21-AI were transformed with the desired plasmids (gRAMP-crRNA1: pGRAMP and pCRISPR-1. gRAMP-crRNA-WT: pGRAMP and pCRISPR-WT. gRAMP-crRNA3: pGRAMP and pCRISPR-3. TPR-CHAT: pTPR-CHAT/pTPR-CHAT H585A C627A. gRAMP complexed with TPR-CHAT (Craspase): pGRAMP-CRISPR-1/pGRAMP-CRISPR-1-target-1 and pTPR-CHAT/pTPR-CHAT H585A C627A) and grown overnight at 37 °C on LB-agar plates containing selection media (50 µg/mL spectinomycin and/or 25 µg/mL chloramphenicol). Colonies were streaked from the plate, resuspended in 100 mL LB containing selection media and grown for ~3 hours before inoculation in 8 L (for overexpression of gRAMP-crRNA and gRAMP complexed with TPR-CHAT (Craspase)) or 4 L (for overexpression of TPR-CHAT) LB medium containing selection media. Cultures were grown at 37 °C and 150 rpm until the cultures reached exponential phase (OD₆₀₀ 0.3-0.5). The grown cultures were incubated on ice for 1 hour and protein expression was induced with a final concentration of 0.2% L-arabinose and 0.5 mM IPTG (for gRAMP-crRNA overexpression) or 1 mM IPTG (for TPR-CHAT and gRAMP complexed with TPR-CHAT (Craspase) overexpression), followed by overnight incubation at 20 °C and 150 rpm. The overnight grown cultures were harvested by centrifugation at 6000 rpm for 30 minutes. The supernatant was discarded and the pellets were resuspended in PBS (50 mL PBS/initial 1 L culture) and harvested by centrifugation

(30 minutes, 3900 rpm 4 °C). The supernatant was discarded, and the pellets stored at -80°C until further use.

Purification of *Sb*-gRAMP-crRNA, *Sb*-gRAMP variants and *Sb*-gRAMP-crRNA complexed with TPR-CHAT (Craspase)

Cell pellets of each 1 L culture were resuspended in 50 mL of ice-cold lysis buffer (100 mM Tris-HCl, 150 mM NaCl, 1 mM DTT, 5% glycerol, pH 7.5). 1 tablet of cOmplete™ EDTA-free Protease Inhibitor Cocktail was added per 50 mL resuspended pellet (except for gRAMP complexed with TPR-CHAT (Craspase)). The cells were lysed with 3 runs at 1000 bar in a cooled French press and spun down at 16000 rpm at 4 °C for 30 min (JA-17 rotor, Avanti). The resulting lysate was filtered through a 0.45 µm syringe filter. To prepare the purification column, a 20 mL gravity column (Bio-Rad) was loaded with 3 mL of a 50% suspension Strep-Tactin®XT Affinity Resin (IBA Lifesciences GmbH) (corresponding with 1.5 mL column bed volume). The Strep-Tactin®XT Affinity Resin was washed with 5 column volumes of ice-cold wash buffer (100 mM Tris-HCl, 150 mM NaCl, 1 mM DTT, 5% glycerol, pH 7.5). The filtered sample lysate was loaded on the washed Strep-Tactin®XT Affinity Resin and subsequently washed with 5 column volumes of ice-cold wash buffer. 10 mL of elution buffer (100 mM Tris-HCl, 150 mM NaCl, 1 mM DTT, 5% glycerol, 50 mM Biotin, pH 7.5) was used to elute the protein. gRAMP D437A D516A, gRAMP D448A, gRAMP D968A and gRAMP D971A were snap frozen and stored at -80 °C until use in the target RNA cleavage assay.

gRAMP-crRNA, gRAMP D448A D516A, gRAMP S457A D516A, gRAMP D698A, gRAMP D698A D771A and gRAMP complexed with TPR-CHAT (Craspase) were subjected to subsequent purification steps. The pooled fractions were gradually diluted 1.5 times with a wash buffer devoid of NaCl (100mM Tris-HCl, 1mM DTT, 5% glycerol, pH 7.5). The sample was spun down at 13,200 rpm at 4 °C for 10 min whereupon the supernatant was transferred to a new tube. For the Heparin affinity chromatography, a 5 mL HiTrap Heparin HP column (Cytiva) was washed with 2 column volumes of degassed MilliQ at 1 mL/min and equilibrated with degassed low salt buffer (100 mM Tris-HCl, 100 mM NaCl, 1 mM DTT, 5% glycerol, pH 7.5) at 1 mL/min. The sample was loaded onto the column and washed with 10 column volumes of ice cold degassed low salt buffer. The proteins were eluted by using a NaCl gradient (0-100% in 25 minutes) from low salt buffer to high salt buffer (100 mM Tris-HCl, 1 M NaCl, 1 mM DTT, 5% glycerol, pH 7.5), collecting 1 mL fractions. Pooled fractions were concentrated (Amicon ultra-4 Centrifugal Filter

Unit with ultracel-100 membrane) and subjected to size exclusion chromatography using Superdex 200 Increase 10/300 GL (Cytiva) column equilibrated with running buffer (100 mM Tris-HCl, 150 mM NaCl, 1 mM DTT, 5% glycerol, pH 7.5) with 0.3 mL/min flow rate using running buffer as mobile phase. For the size exclusion chromatography of *Sb*-gRAMP-crRNA and *Sb*-gRAMP-crRNA complexed with TPR-CHAT prior to SEC-MALS analysis, running buffer without glycerol (100 mM Tris-HCl, 150 mM NaCl, 1 mM DTT, pH 7.5) was used. Pooled fractions were concentrated, snap frozen in liquid nitrogen and stored at -80 °C until further use.

Purification of TPR-CHAT

Cell pellets were unfrozen and resuspended in 200 mL of ice-cooled lysis/wash buffer (100 mM Tris-HCl, 150 mM NaCl, 1 mM DTT, 5% glycerol, 25 mM imidazole, pH 7.5). Cell lysis was performed three times in a cooled French press (1 kbar). The lysate was centrifuged at 16,000 rpm for 30 minutes at 4 °C. The supernatant was filtered through a 0.45 µm syringe filter and loaded on a disposable 20 mL column (Bio-Rad) for gravity-flow affinity chromatography containing HIS-Select Nickel Affinity Gel (500 µL/50 mL lysate) (Sigma-aldrich) that was washed with 20 mL of ice-cold lysis/wash buffer. The loaded column was washed with 15 mL of ice-cold lysis/wash buffer. The protein was eluted with ice-cold elution buffer (100 mM Tris-HCl, 150 mM NaCl, 1 mM DTT, 5% glycerol, 250 mM imidazole, pH 7.5). Pooled fractions were concentrated, snap frozen in liquid nitrogen and stored at -80 °C until further use.

RNA extraction

50 µL of purified *Sb*-gRAMP-crRNA (~1 mg/mL) or gRAMP complexed with TPR-CHAT (Craspase) (~0.6 mg/mL) were thawed and incubated with 3 µL of 800 units/mL proteinase K (New England Biolabs) at 37 °C for 1 hour to digest the protein content, followed by heat inactivation at 95 °C for 5 minutes. To separate the RNA from the digested protein content, acidic phenol (pH 4.5, phenol:chloroform = 5:1, Invitrogen) was added to the sample in a 1:1 ratio, vortexed for 1 minute and centrifuged for 10 minutes at 13200 rpm at room temperature. The aqueous phase was collected and subjected to RNA precipitation (20 µL 3M NaAcetate and 500 µL 100% ethanol per 200 µL of sample) for 1 hour at -20 °C. Samples were spun down at 13,200 rpm at 4 °C for 2 hours, washed twice with ice-cold 70% ethanol and spun down at 13,200 rpm at 4 °C for 10 minutes. The pellet was dried in a SpeedVac concentrator (Thermo Fisher Scientific) for 30 minutes at 60 °C and resuspended in RNA grade water. Samples were stored at -80 °C until

further use. For RNA digestion, 10 μ L of \sim 50 ng/ μ L extracted RNA was incubated with 1 μ L of 20 mg/mL RNase A (Thermo Fisher Scientific) for 30 minutes at 37 $^{\circ}$ C. Visualization of RNA was done by mixing 10 μ L sample of \sim 50 ng/ μ L with 10 μ L 2x RNA loading dye (95% formamide, 0.025% SDS and 0.5 mM EDTA) and running the sample on an 8M urea 10% PAGE gel with the Low Range ssRNA Ladder (New England Biolabs). The gel was stained with Sybr Gold and imaged on a Typhoon laser-scanner platform (Cytiva).

RNAseq of purified RNA

RNA sequencing was performed on RNA extracted from *Sb*-gRAMP-crRNA-WT. 10 μ g of phenol-chloroform extracted RNA was incubated with 22 U T4 Polynucleotide Kinase (PNK) (New England Biolabs) and 1x PNK buffer (New England Biolabs) for 4 hours at 37 $^{\circ}$ C for 2'-3'-dephosphorylation. Subsequently, another 10 U PNK and 1 mM ATP was added for 1.5 hours at 37 $^{\circ}$ C for 5'-phosphorylation before heat inactivation at 65 $^{\circ}$ C for 20 minutes. PNK treated samples were subjected to another round of phenol-chloroform purification prior to sending for small RNA sequencing (Macrogen). The small RNA library was prepared using the Illumina TruSeq RNA Library Prep Kit with 20% PhiX and 10% miRNA control added. A HiSeq X lane (2x150bp) sequencing run was performed. The obtained reads (2,649,538 in total) were trimmed using cutadapt (26) to remove the adapters. The single reads of size 40 to 60 (954,096 in total) were filtered and mapped on the CRISPR array sequence using minimap2 (27).

SDS-PAGE analysis

20 μ L of protein sample was supplemented with 5 μ L of 5X Laemmli buffer (375 mM Tris-HCl, 9% SDS, 50% glycerol, 0.03% bromophenol blue) and 2.5 μ L 1 M DTT. Samples were incubated at 95 $^{\circ}$ C for 10 minutes before loading on a 4-20% Mini-Protean TGX Precast Gel (Bio-Rad) with PageRuler Prestained Protein Ladder (10 to 180 kDa) or PageRuler Plus Prestained Protein Ladder (10 to 250 kDa). Gels were run in 1X TGS buffer (25 mM Tris-HCl, 192 mM glycine, 0.1% SDS) at 200 V for 30-45 minutes, washed in MilliQ water and stained for 1 hour with BioSafe Coomassie G-250 stain (Bio-Rad) under continuous shaking. Gels were washed in MilliQ water for 30 minutes before imaging.

Target RNA cleavage

RNA cleavage reactions were performed in 10 μ L reaction volume, containing purified 200 nM *Sb*-gRAMP-crRNA or *Sb*-gRAMP-crRNA1 complexed with TPR-CHAT (Craspase), 100 nM Cy5-labelled RNA oligo, 11 mM Tris-HCl, 67 mM NaCl, 4.5 mM DTT and 1 mM MgCl₂ unless stated otherwise. Typical reactions were incubated at 20 °C for 2 hours, after which 0.5 μ L of 800 units/mL proteinase K (New England Biolabs) was added for 1 hour at 37 °C and 95 °C for 5 minutes to stop the reactions. 5 μ L of the reaction was mixed with 5 μ L of 2x RNA loading dye (95% formamide, 0.025% SDS and 0.5 mM EDTA) and loaded on an 8M urea 10% PAGE gel (pre-run at 350 V for 1 hour, sample run at 333V for 2 hours) with 100 nM ladder containing 5'-Cy5 labelled RNA oligo's of sizes 10, 20, 30, 40, 50 and 60 nt (table S5). Gels were imaged on a Typhoon laser-scanner platform (Cytiva).

Biochemical characterization of the RNA ends of gRAMP cleavage products

In order to characterize the chemical 5'- and 3'-ends of the cleavage products generated by *Sb*-gRAMP, cleavage reactions were heat inactivated at 95 °C for 5 minutes and subsequently treated with Antarctic phosphatase (for 5' and 3' dephosphorylation) or T4 PNK (for 5' phosphorylation and 2'-3'-dephosphorylation). For phosphatase treatment, 1.1 μ L 10x Antarctic phosphatase reaction buffer (New England Biolabs) and 0.5 μ L of 5,000 units/mL Antarctic phosphatase (New England Biolabs) was added and incubated for 30 minutes at 37 °C. For T4 PNK treatment, 1 μ L of 10,000 units/mL T4 PNK (New England Biolabs), 1 μ L 10 mM ATP and 1 μ L 10x T4 PNK buffer (New England Biolabs) was added and incubated for 30 minutes at 37 °C. Reactions were inactivated at 95 °C for 5 minutes, whereupon 0.5 μ L of 800 units/mL proteinase K (New England Biolabs) was added and incubated for 30 minutes at 37 °C, followed by inactivation at 95 °C for 5 minutes. For visualization, 10 μ L of the reaction was mixed with 2x RNA loading dye (95% formamide, 0.025% SDS and 0.5 mM EDTA) and loaded on an 8M urea 10% PAGE gel (pre-run at 350 V for 1 hour, sample run at 333V for 2 hours). Gels were imaged on a Typhoon laser-scanner platform (Cytiva).

SEC-MALS

The gRAMP-crRNA1, gRAMP-crRNA3 and gRAMP complexed with TPR-CHAT (Craspase) samples for SEC-MALS were prepared by pooling the SEC elutions corresponding to the protein peaks (10-11 mL for gRAMP-crRNA1 and 9.5-10.5 mL for Craspase). Samples were injected at final concentrations of 1.2 mg/mL (gRAMP-crRNA1), 1.0 mg/mL (gRAMP-crRNA3)

and 0.6 mg/mL (Caspase) in running buffer (100 mM Tris-HCl, 150 mM NaCl, 1 mM DTT, pH 7.5) onto a Superdex 200 Increase 10/300 GL (Cytiva). After SEC, the sample passed a DAWN HELEOS 8 light scattering instrument (Wyatt) and a Optilab T-rEX refractive index detector (Wyatt). Light source of the RI detector and wavelength of the laser in the light scattering instrument were 658 and 660 nm, respectively. Molecular mass distribution and concentrations of chromatogram peaks were calculated based on the light scattering signal and the refractive index, respectively, derived from peak half-height regions (9.87-10.43 mL for gRAMP-crRNA1, 9.76-10.39 mL for gRAMP-crRNA3 and 9.62-10.10 mL for gRAMP complexed with TPR-CHAT (Caspase)). For molar mass calculations, ASTRA 7.3.2 software (Wyatt) with the protein conjugate analysis module was used with refractive-index increments (dn/dc) of 0.1850 mL/g (protein) and 0.1680 mL/g (RNA). Protein UV extinction coefficients of 1.203 mL $mg^{-1} cm^{-1}$ (gRAMP-crRNA1 and gRAMP-crRNA3) and 1.225 mL $mg^{-1} cm^{-1}$ (gRAMP complexed with TPR-CHAT (Caspase)), and RNA UV extinction coefficients of 15.3914 mL $mg^{-1} cm^{-1}$ (gRAMP-crRNA1 and gRAMP complexed with TPR-CHAT (Caspase)) and 15.8769 mL $mg^{-1} cm^{-1}$ (gRAMP-crRNA3) were used. UV extinction coefficients were estimated using ExPASy ProtParam (<https://web.expasy.org/protparam/>) (28) and MolBioTools DNA calculator (www.molbiotools.com) using the sequences for gRAMP and TPR-CHAT. For the RNA of gRAMP-crRNA1 and gRAMP complexed with TPR-CHAT (Caspase), the UV extinction coefficient was calculated using 55 nt ssRNA of crRNA1 (AAACAAGAGAAGGACUAAUGUCACGGUACCCAAUUUCUGCCCCGGACUCCAC G) with 5' phosphate. For the RNA of gRAMP-crRNA3, the UV extinction coefficient was calculated using 55 nt ssRNA of crRNA3 (AAACAAGAGAAGGACUAAUGUCACGGUACAAUUAUCAUUUGGACAGCUUCCU C) with 5' phosphate.

In-gel proteolytic digestion and protein identification by mass spectrometry

To identify the purified proteins, SEC purified gRAMP complexed with TPR-CHAT (Caspase) elutions were analyzed using SDS-PAGE (fig. S19B, elution 11), whereupon the bands of interest (upper band, ~214 kDa and lower band, ~83 kDa) were cut from the gel and minced into small pieces using a sterile scalpel. Gel pieces were destained using Coomassie destaining solution (100 mM ammonium bicarbonate in 40% acetonitrile) for 15 minutes at 37 °C and shaking at 300 rpm. A reduction was performed using 200 μ L of reducing agent (10 mM dithiothreitol)

and incubation for 30 minutes at 56 °C. After removal of the reducing agent and cooling down of the gel pieces to room temperature, 200 µL of alkylating solution (55 mM iodoacetamide) was added and incubated in the dark at room temperature for 30 minutes. After removal of the alkylation solution, 200 µL of Coomassie destaining solution was added and incubated for 5 minutes at room temperature with 300 rpm shaking. The solution was discarded and 200 µL of acetonitrile (100%) was added and incubated for approximately 10 minutes at room temperature until the gel pieces were dehydrated. Proteolytic in-gel digestion was initiated by adding 2 µL of a 100 ng/µL trypsin solution (Promega, sequencing grade) dissolved in 100 mM ammonium bicarbonate buffer. After 5 minutes, an additional 50 µL of 100 mM ammonium bicarbonate buffer was added to ensure full coverage of the gel pieces. Samples were incubated overnight at 37 °C with 300 rpm shaking. The next day, samples were spun down and 150 µL of extraction solution (70% acetonitrile, 5% formic acid) was added to the supernatant and incubated for 15 minutes at 37 °C with 300 rpm shaking. The supernatant was collected, 100 µL of acetonitrile (100%) was added and incubated for 15 minutes at 37 °C with 300 rpm shaking. Next, 100 µL of 10:90 (v/v) acetonitrile:water was added to the samples and incubated for 15 minutes at 37 °C with 300 rpm shaking. The supernatant was collected and dried using a SpeedVac concentrator (Thermo Fisher Scientific).

Before spectrometry analysis, the dried samples were resuspended in 15 µL resuspension buffer (3% acetonitrile, 0.1% formic acid) under careful vortexing. An aliquot corresponding to approximately 100 ng protein digest was analyzed using a nanoLC (EASY 1200, Thermo Fisher Scientific) coupled online to a QE plus Orbitrap mass spectrometer (Thermo Fisher Scientific), which was operated in data-dependent acquisition (DDA) mode, acquiring MS2 spectra of the top 10 signals (29). Mass spectrometric raw data were analyzed using PEAKS Studio X (Bioinformatics Solutions Inc., Canada) by comparing the obtained peptide fragmentation spectra to a constructed *E. coli* BL21(DE3) database (retrieved from the UniProtKB database, www.uniprot.org) merged with the gRAMP and TPR-CHAT protein sequences, thereby considering 20 ppm parent mass error, 0.2 Da fragment mass error, 2 missed cleavages, carbamidomethylation as fixed, and oxidation and deamidation as variable peptide modifications. Peptide matches and protein identification were filtered for 1% false discovery rate. Protein identification with >1 unique peptide sequences were considered as confident matches.

Complex dissociation test

Purified gRAMP complexed with TPR-CHAT (Craspase) (0.1 μ M) was incubated with ~6.6-fold excess of complementary ssRNA (Target 2) (0.66 μ M). The mixture was incubated for 2 hours at 20 °C and then loaded into a Superdex 200 Increase 10/300 GL (Cytiva) previously equilibrated with running buffer (100 mM Tris-HCl, 150 mM NaCl, 1 mM DTT, 5% glycerol, pH 7.5). Fractions were collected and analyzed on an SDS-PAGE gel.

Growth experiments

Electrocompetent *E. coli* BL21-AI cells were transformed by electroporation with the desired plasmids. Individual colonies for each condition (pGRAMP-CRISPR-1, pGRAMP-CRISPR-1-target-1, pTPR-CHAT, pTPR-CHAT H585A C627A, or combinations) were inoculated in 10 mL of LB supplemented with appropriate antibiotic(s) and incubated overnight at 37 °C and 180 rpm. Overnight cultures were diluted to OD₆₀₀ of 0.05 after which 200 μ l was plated in a 96-well plate in duplicate. The cultured plate was incubated at 37 °C in a Synergy™ H1 microplate reader (BioTek) for 1.5 hours. Protein expression was induced with a final concentration of 0.2% L-arabinose and 1 mM IPTG, followed by incubation at 20 °C with shaking. OD₆₀₀ was measured every 10 minutes.

To verify target RNA expression, two cultures per condition (starting with three colonies) were grown in LB supplemented with appropriate antibiotic(s) at 37 °C and 180 rpm. Upon reaching OD₆₀₀ of approximately 0.45, expression was induced for 3 hours using 1 mM IPTG and 0.2% L-arabinose. Total RNA was extracted with the mirVana RNA Isolation Kit (Thermo Fisher Scientific) using the total RNA protocol, with acidic phenol (Invitrogen) according to manufacturer's instructions. Contaminant DNA was removed using TURBO DNA-free kit (Thermo Fisher Scientific) according to manufacturer's instructions. ~100 ng of treated RNA was reverse transcribed using the GoTaq 2-Step RT-qPCR system (Promega) and random primers according to manufacturer's instructions. Control reactions were prepared without reverse transcriptase. The resultant cDNA was used in PCR reactions with GoTaq qPCR Master Mix (Promega) and primers amplifying the target RNA (BN3596 and BN3599; 137 bp), spectinomycin resistance gene (aminoglycoside adenylyltransferase; *aadA*) RNA (BN3642 and BN3643; 146 bp) as internal plasmid RNA control, or caseinolytic peptidase B (*clpB*) RNA (BN3649 and BN3650; 157 bp) as internal genomic RNA control, at 95 °C for 2 min followed by 25 cycles of denaturation at 95 °C for 15 seconds and annealing and extension at 60 °C for 1 minute. PCR

reactions were run on 2% agarose gels and stained with SYBR Safe (Thermo Fisher Scientific) for visualization of nucleic acids.

RNase T1 ladder generation

5 For exact cleavage site determination, cleavage products were compared to a ladder consisting of RNase T1 digested target RNA. To generate the ladder, ~20 ng of Target 2 or Target 7 was combined with ~140 ng of *E. coli* RNA that was extracted with the mirVana RNA Isolation Kit (Thermo Fisher Scientific) using the total RNA protocol. Subsequently, 0.1 U of RNase T1 (Thermo Fisher Scientific) was added and incubated for 1 minute at 37 °C, followed by addition
10 of 1.6 U of Proteinase K (New England Biolabs) and incubation for 30 minutes at 37 °C. Heat inactivation was performed for 5 minutes at 95 °C whereupon 2x RNA loading dye (95% formamide, 0.025% SDS and 0.5 mM EDTA) was added. The samples were stored at -20 °C until use.

Type III-E bioinformatics mining

15 For the identification of assemblies containing gRAMP, earlier reported gRAMPs (5) were used as seed in the non-redundant NCBI database (available from: <https://www.ncbi.nlm.nih.gov>), MGNIFY database (available from: <https://www.ebi.ac.uk/metagenomics>) and IMG databases (available from: <https://img.jgi.doe.gov>) on January 13th, 2021. Mmseqs2 easy-cluster was used
20 to find gRAMP homologs based on 60% coverage of the earlier reported gRAMPs with a minimum sequence identity of 25% (30). Genes of discovered contigs were annotated using hhpred using default settings (31). Only gRAMPs containing a co-occurring TPR-CHAT were included in further analyses.

Spacer analysis and strand bias determination

25 Type III-E spacers were collected from previously characterized type III-E systems (32). Additional spacers from metagenomes (JAABRU010000211.1, JPDT01002993.1, JPDT01002663.1, JPDT01002993.1 and JPDT01000635.1) were found based on similarity to repeat sequences from already described arrays and a complete genome of *Desulfonema magnum*
30 (NZ_CP061800.1) also contained additional spacers. Matches in (meta)genomes to these spacers were subsequently found using BLAST as previously described (33). Hits were removed when found within arrays or with nucleotide identity <90% (no gaps allowed). Two hits from

MVRP01000104.1 that were below the 90% were still included based on the low possibility that these hits would occur at random in the same metagenome (e-value $<10^{-6}$). The potential MGE origin of type III-E spacer matches in metagenomes was determined by analyzing and annotating flanking genes of spacer matches using prokka (34). If one of the genes were determined to be characteristic of viruses (e.g. viral proteins), transposons (e.g. transposases) or plasmids (e.g. conjugation machinery), the hit with the spacer match was predicted to be of MGE origin. Strand bias was determined by comparing the orientation of the spacer compared to the orientation of open reading frames predicted on the matching target using Prodigal (33, 35).

Phylogenetic tree construction

All Cmr4 and Csm3 protein sequences were downloaded from Interpro on May 19th, 2021, and clustered with the gRAMP proteins. The phylogenetic tree was constructed as previously described (25). In short, cd-hit v4.8.1 (36) was used to filter redundant proteins. The remaining proteins were aligned using MAFFT v7.475 linsi (37) and Trimal v1.4.rev15 (38) was used to remove columns composed of gaps (-nt 0.95). Tree visualization was done by IQ-TREE v2.1.2 (39) using 1000 bootstraps. To find out to which CRISPR-Cas type the Cmr4 and Csm3 proteins belonged, each protein was blasted onto the NCBI database. In case of an exact hit, the contig in which the hit was found was analyzed using CRISPRCasTyper (32). The final phylogenetic tree was visualized using figtree v1.4.4 and iTol (40).

Supplementary Text

Nucleic acid content calculation

5 The molar mass determined for the nucleic acid content of the *Sb*-gRAMP-crRNA1 during SEC-MALS is $16.8 \pm 13.9\%$ kDa, or 14.46-19.14 kDa. Approximating the molar mass of an average ribonucleotide monophosphate at 320.5 Da and 5'-phosphate at 79 Da, 14.46 kDa corresponds to $(14,460-79.0)/320.5 = 44.9$, or 45 nucleotides and 19.14 kDa corresponds to $(19,140-79.0)/320.5 = 59.5$, or 60 nucleotides. This presents a range for ssRNA (45-60 nt) bound to *Sb*-gRAMP.

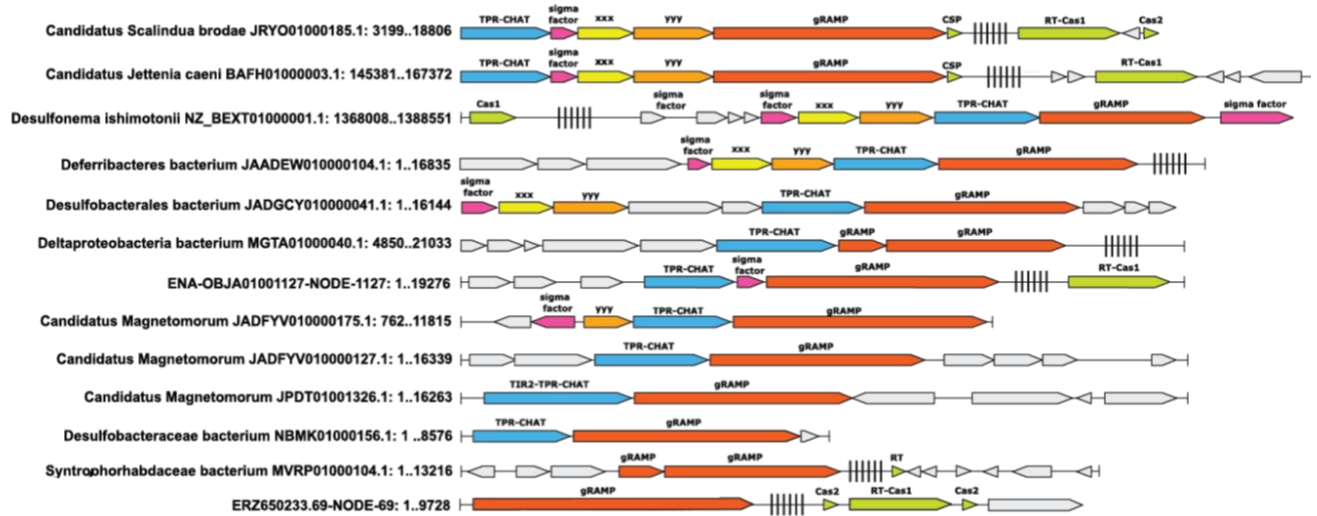


Fig. S1. Identified CRISPR-Cas type III-E loci. Typical type III-E components include gRAMP (red), TPR-CHAT (blue), RpoE sigma factor (pink) and two genes of unknown function (xxx in yellow, yyy in light orange (5)). Canonical CRISPR-Cas proteins are annotated in green. CRISPR arrays are indicated with staggered vertical lines. Start and ends of contigs are indicated with single vertical lines at the ends.

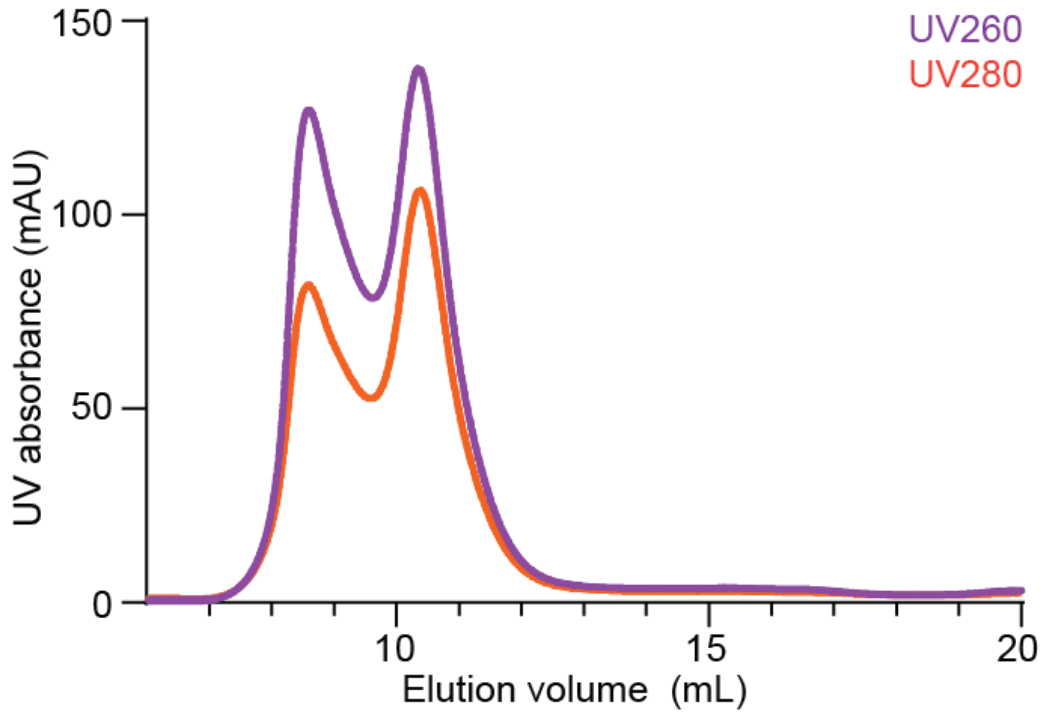


Fig. S2. UV absorption peaks at 260 nm (purple) and 280 nm (orange) after size-exclusion chromatography (SEC) (Superdex 200 Increase 10/300 GL) of purified *Sb*-gRAMP that was expressed in the presence of a plasmid containing five copies of the first spacer from the native *Candidatus* “*Scalindua brodae*” CRISPR array.

5

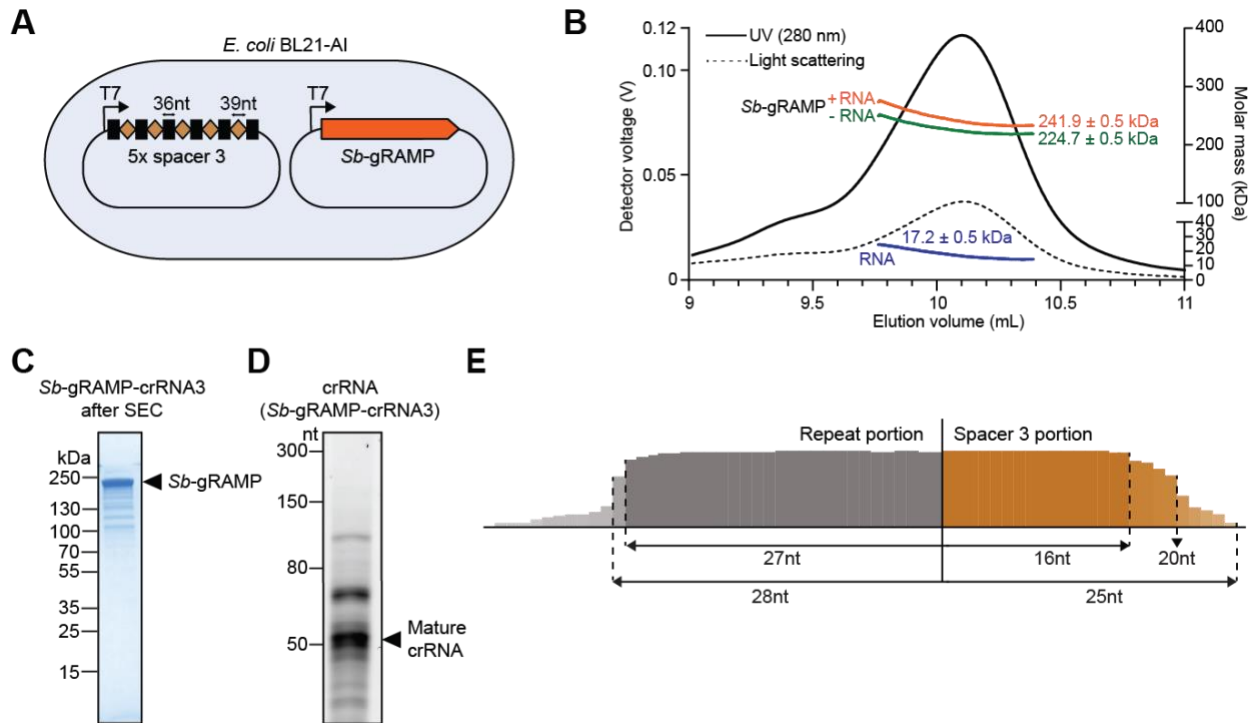


Fig. S3. Protein purification and RNA characterization of *Sb-gRAMP* expressed in the presence of a CRISPR array derived from spacer 3 (*Sb-gRAMP-crRNA3*). **(A)** Schematic showing the heterologous expression system used for *Sb-gRAMP-crRNA3* overexpression. **(B)** SEC-MALS peaks corresponding to light scattering and UV₂₈₀ absorbance profiles of purified *Sb-gRAMP-crRNA3*. The molar masses are derived from the peak half-height region (9.8-10.4 mL). **(C)** SDS-PAGE analysis after SEC. **(D)** Denaturing urea PAGE analysis of the nucleic acid content in *Sb-gRAMP-crRNA3*. **(E)** RNAseq read depth of repeat-spacer 3 with predominant repeat and spacer lengths indicated based on consensus processing (fig. S6B).

RNA extracted from
Sb-gRAMP-crRNA-WT

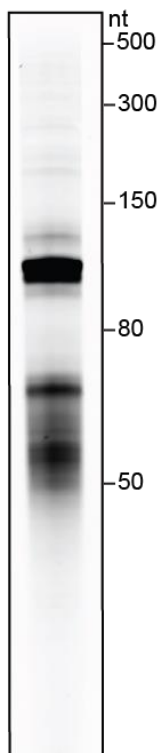


Fig. S4. RNA extracted from *Sb-gRAMP* expressed with the native *Candidatus* “*Scalindua brodae*” CRISPR array (*Sb-gRAMP-crRNA-WT*) after heparin chromatography. The extracted RNA was subsequently used for RNAseq.

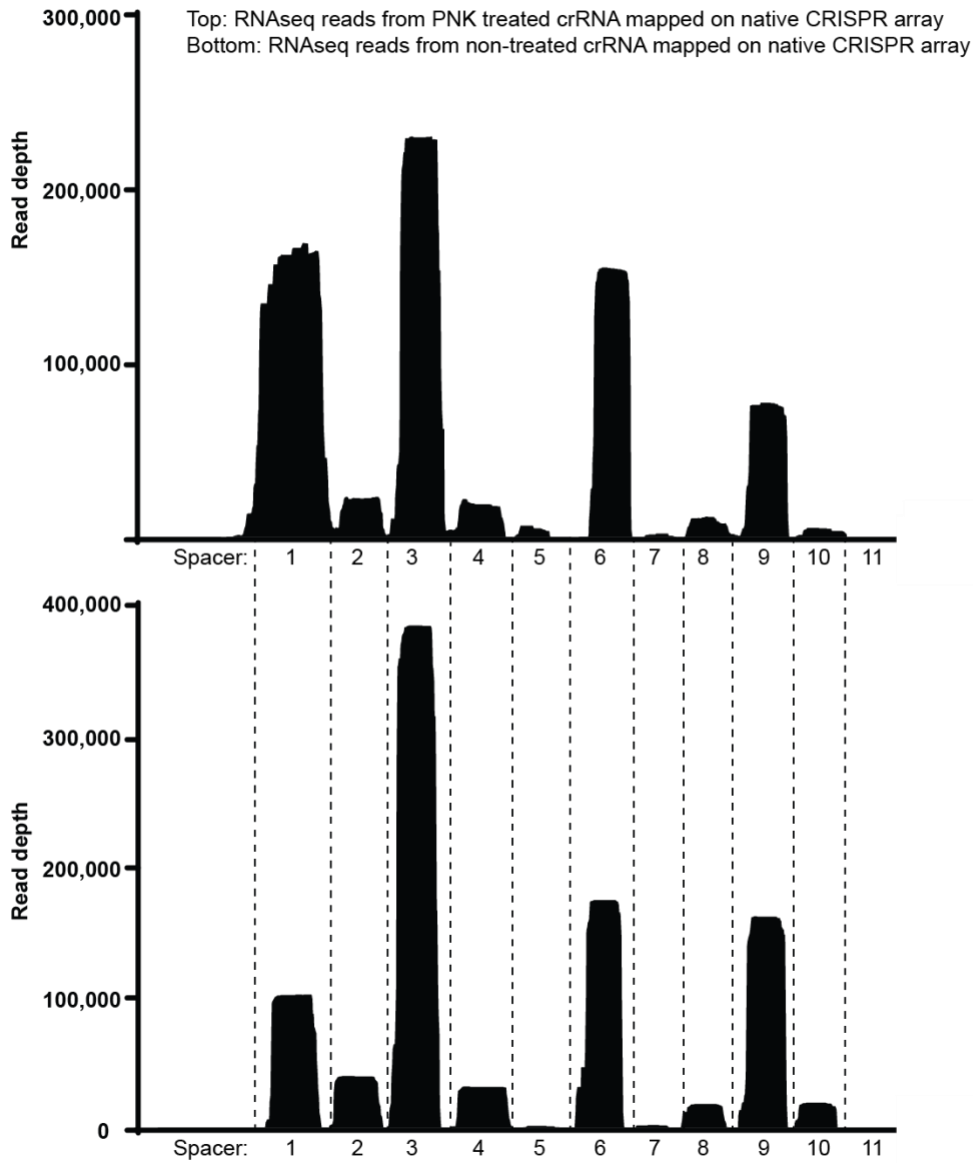


Fig. S5. RNAseq read depth of mature crRNA (40 to 60 nt), with (top) or without (bottom) prior T4 Polynucleotide Kinase (PNK) treatment. Both sequence read sets are mapped on the native CRISPR array of *Candidatus* “*Scalindua brodae*”. RNAseq protocols require 5'-P and 3'-OH for appropriate adapter ligation to the RNA. PNK is capable of adding a 5'-phosphate and removing a cyclic 2'-3'-phosphate, thereby ensuring crRNA termini suitable for RNAseq.

5

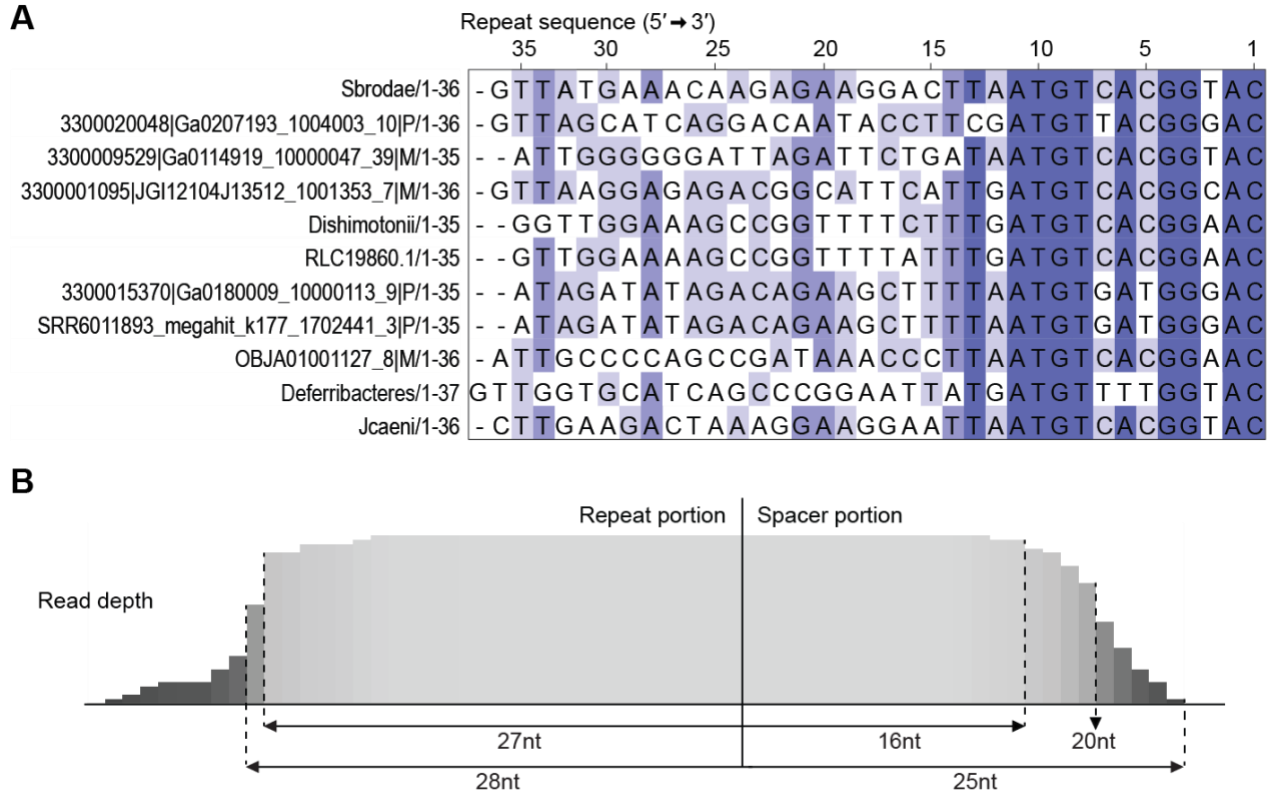


Fig. S6. *Candidatus* “*Scalindua brodae*” native CRISPR array analysis. **(A)** Alignment of repeats found in various type III-E loci with the consensus nucleotide per position colored on occupancy in the alignment, from white (no consensus nucleotide) to dark (complete or near-complete occupancy of the consensus nucleotide). The alignment was generated using the Cobalt multiple alignment tool (41) with default settings and visualized using Jalview (42) **(B)** Read depth of the repeat and spacers with 10,199 reads in which all repeat-spacer pairs are represented. Consensus processing sites are indicated.

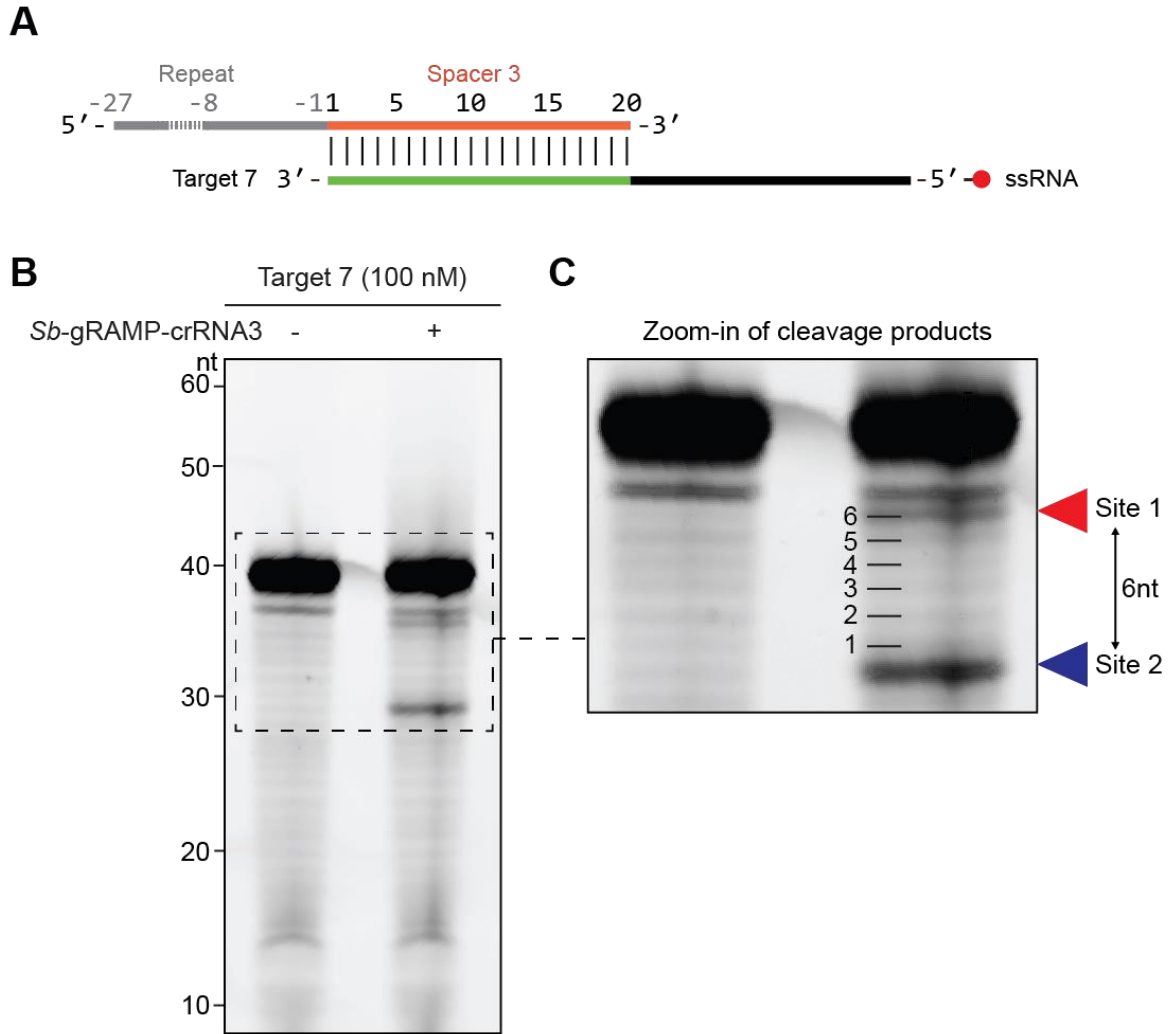


Fig. S7. *Sb*-gRAMP-crRNA3 cleaves cognate target ssRNA. (A) Outline of the Cy5-labelled RNA target tested for activity of *Sb*-gRAMP loaded with crRNA derived from spacer 3 in the native *Candidatus* “*Scalindua brodae*” CRISPR array (*Sb*-gRAMP-crRNA3). Substrate details are listed in table S5. (B) Denaturing urea PAGE gel of cleavage reactions consisting of 200 nM *Sb*-gRAMP-crRNA3 incubated with cognate Target 7. (C) Zoom-in of the cleavage products with single nucleotide steps in the auto-hydrolysis ladder indicated.

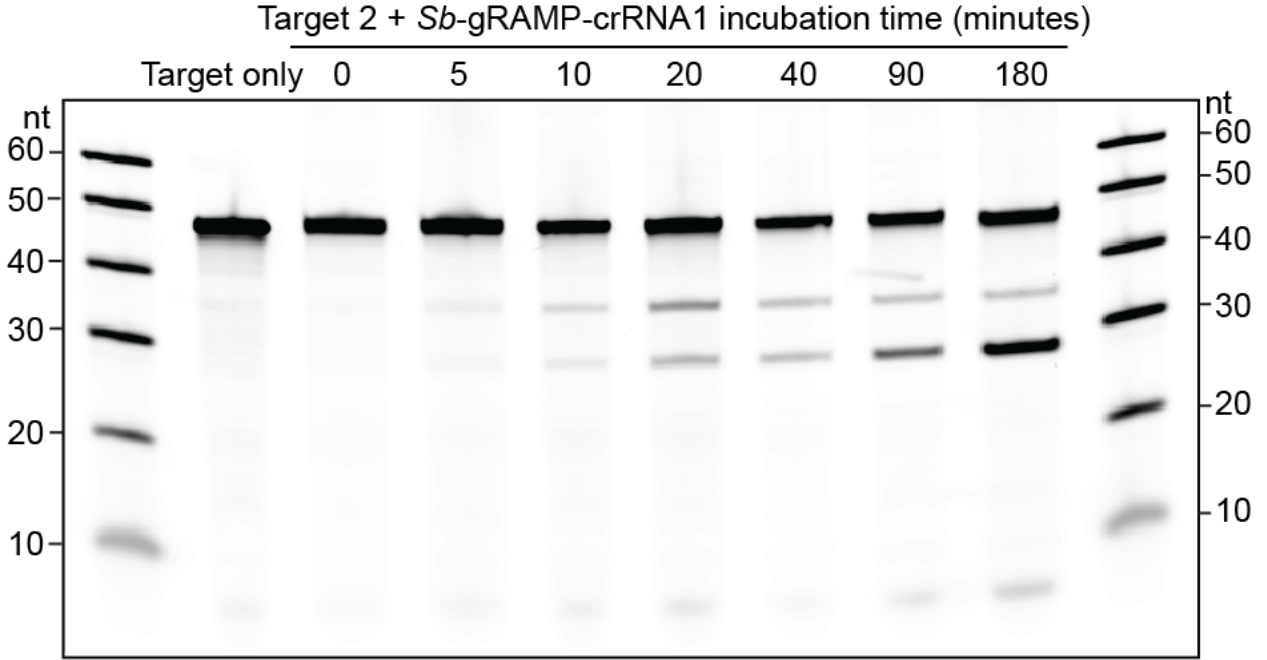


Fig. S8. *Sb*-gRAMP-crRNA1 incubation with complementary ssRNA over time. Denaturing urea PAGE gel of cleavage reactions consisting of *Sb*-gRAMP-crRNA1 and cognate Target 2 with different incubation times. Substrate details are listed in table S5.

5

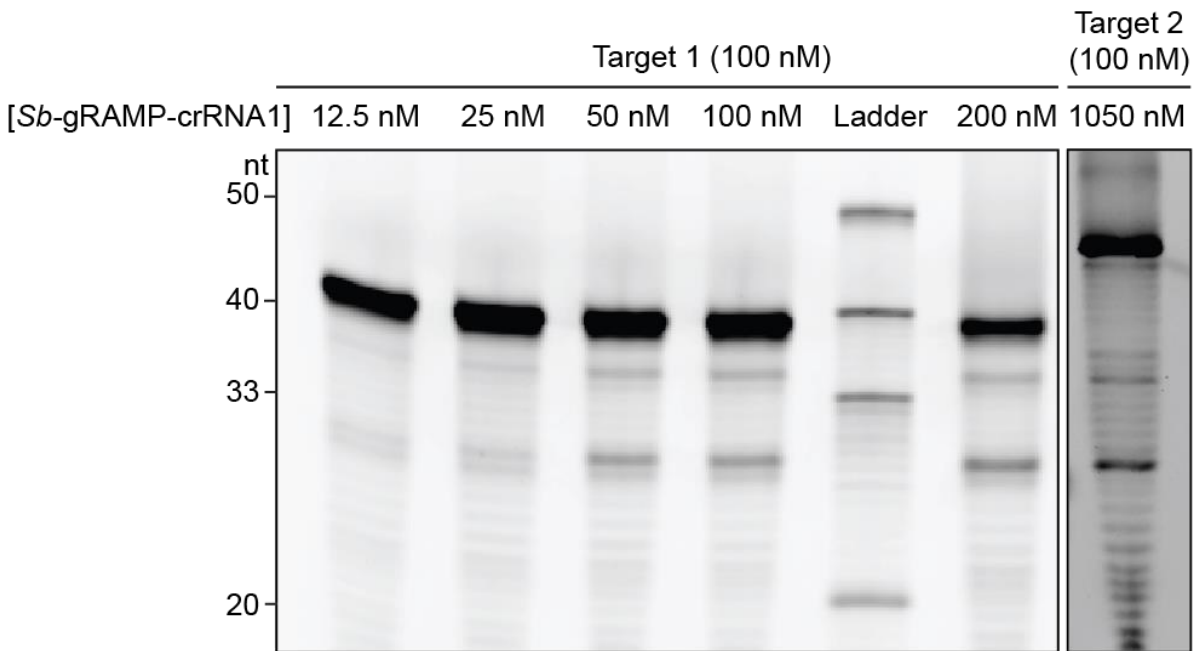


Fig. S9. Target RNA cleavage by *Sb*-gRAMP-crRNA1 proceeds with a limited substrate turnover. Denaturing urea PAGE gel of cleavage reactions consisting of different *Sb*-gRAMP-crRNA1 concentrations with 100 nM cognate Target 1 and Target 2. Substrate details are listed in table S5.

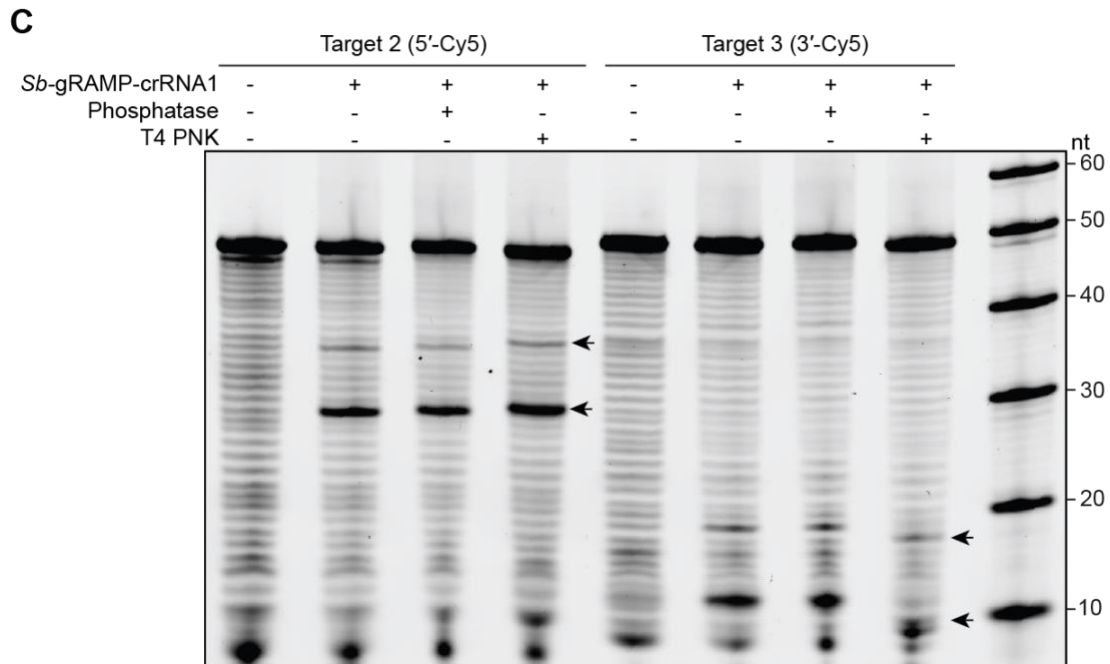
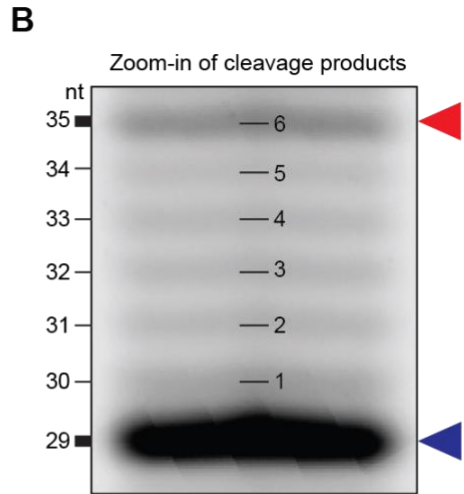
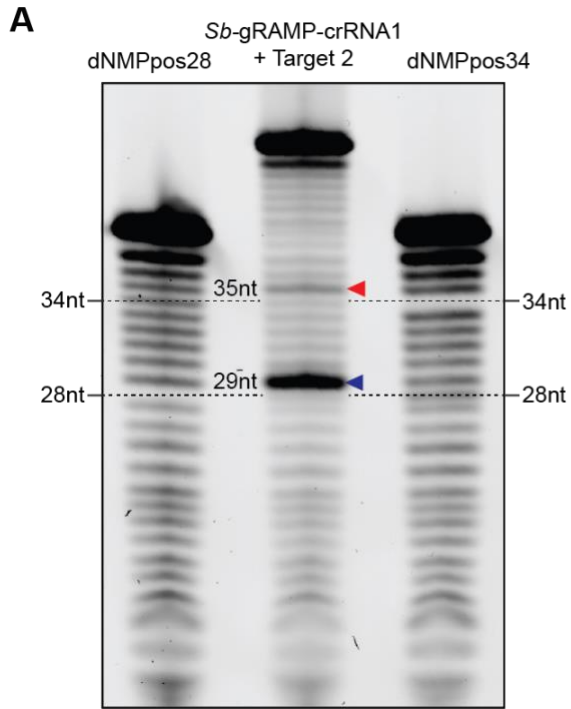


Fig. S10. *Sb*-gRAMP-crRNA1 and *Sb*-gRAMP-crRNA3 exact cleavage positions in target RNA. (A) Determination of the cleavage sites using the auto-hydrolysis products from the target RNA and the internal absence of an auto-hydrolysis product in ssRNA oligo's due to a deoxyribonucleoside monophosphate (dNMP) at position 28 (dNMPpos28) or position 34 (dNMPpos34). The absence of a 2'-OH at dNMP prevents the nucleophilic attack on the 3' adjacent phosphorus in the phosphodiester bond and hence prevents the appearance of an auto-hydrolysis product of that size. Cleavage products are indicated with the red and blue arrowheads and are 29 nt and 35 nt. Substrate details are listed in table S5. (B) Zoom-in of the cleavage products generated by *Sb*-gRAMP-crRNA1 with counting steps in the auto-hydrolysis ladder. Cleavage products are indicated with arrowheads. (C) Cleavage products of cognate target RNA Cy5-labelled 5' (Target 2) or 3' (Target 3) after incubation with Antarctic phosphatase and T4 polynucleotide kinase (PNK). Treatment of Target 2 with PNK resulted in an upwards shift (indicated by the arrows) of the cleavage products, suggesting the removal of a 3'-phosphate. Conversely, treatment of Target 3 with PNK resulted in a marked downward shift (indicated by the arrows), indicating the addition of a 5'-phosphate. These results indicate that cleavage products generated by *Sb*-gRAMP-crRNA1 carry 5'-OH and 3'-P, allowing comparison with auto-hydrolysis products in (A), as the chemical nature of hydrolysis products is also 5'-OH and 3'-P and thus comparable in electrophoretic mobility. (D) Determination of the cleavage sites using RNase T1 digested target RNA as a ladder. RNase T1 cleaves the phosphodiester bond of single-stranded RNA between 3'-guanylic residues and the 5' of the adjacent nucleotides. RNase T1 cleavage sites of Target 2 (cognate to crRNA1) and Target 7 (cognate to crRNA3) are indicated with black arrowheads and the size is indicated in nt. Cleavage products are indicated with the red and blue arrowheads and are 29 nt and 35 nt for *Sb*-gRAMP-crRNA1, and 30 nt and 36 nt for *Sb*-gRAMP-crRNA3. Target 7 is 1 nt longer (due to a 1 nt longer native spacer) at the 5' (where the Cy5 label is positioned) compared to Target 2 (E), so the observed one nucleotide difference in cleavage products for *Sb*-gRAMP-crRNA1 and *Sb*-gRAMP-crRNA3 indicates that the same positions are cleaved relative to the crRNA. This demonstrates that target RNA cleavage is position specific.

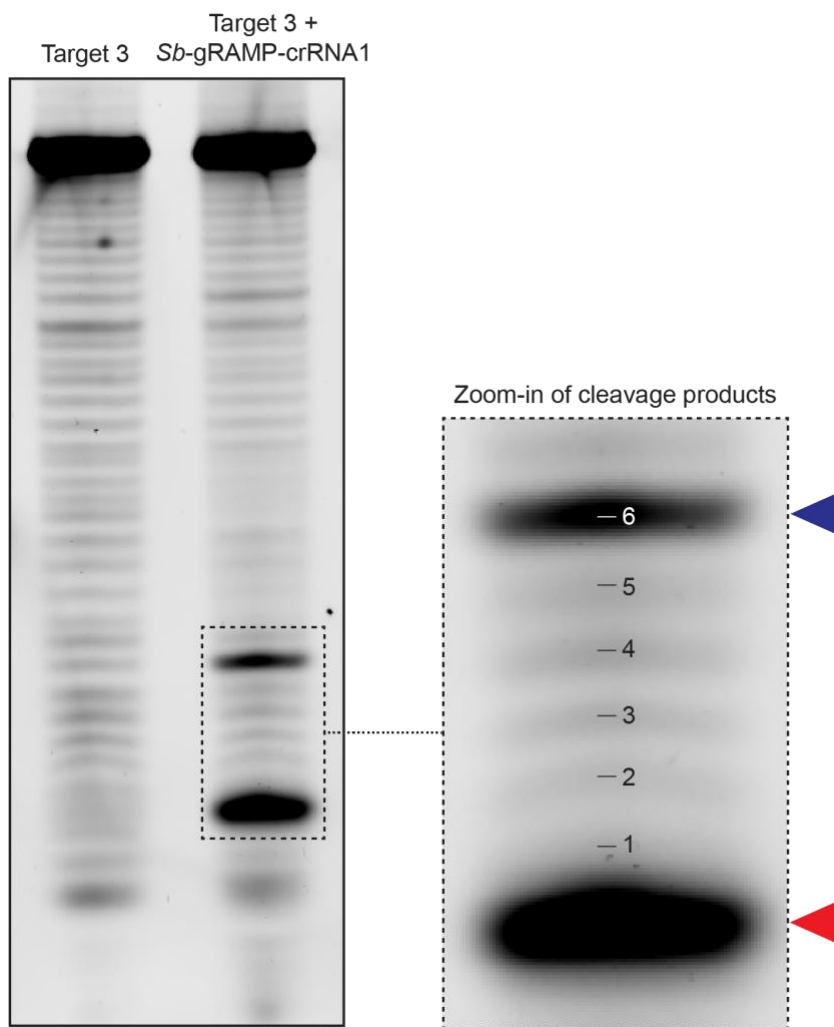


Fig. S11. *Sb*-gRAMP-crRNA1 cleavage products of Target 3 are 6 nt apart. Denaturing urea PAGE gel of Target 3 incubated with *Sb*-gRAMP-crRNA1 with a zoom-in of the cleavage products (indicated with arrowheads) in which nucleotide counting steps are indicated.

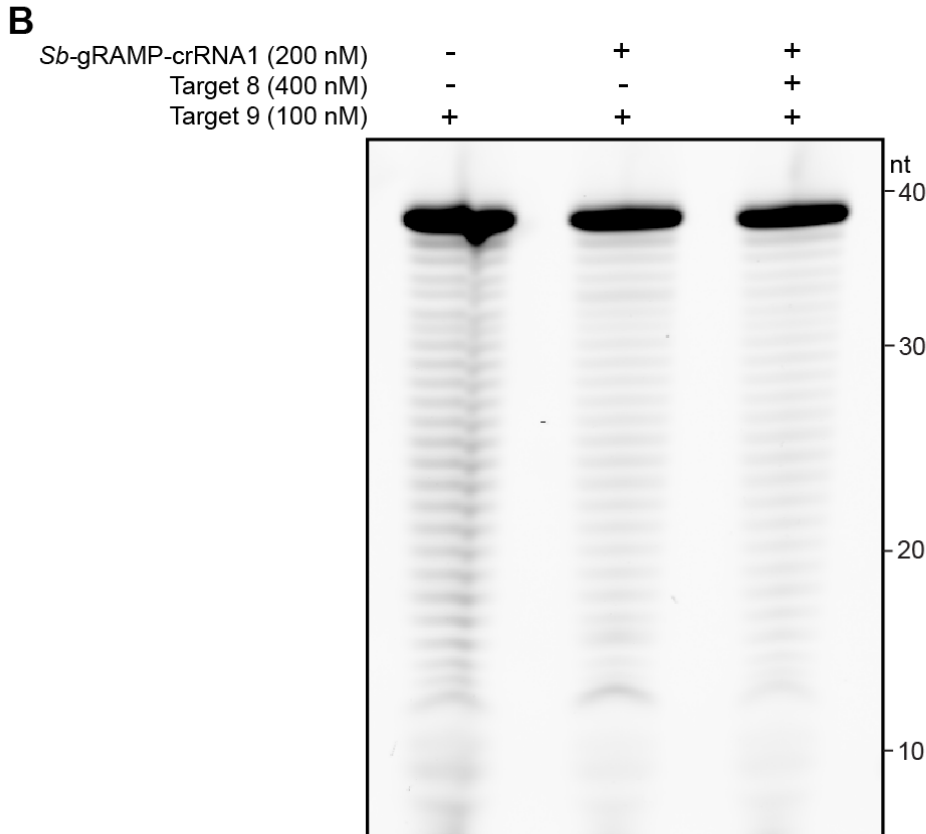
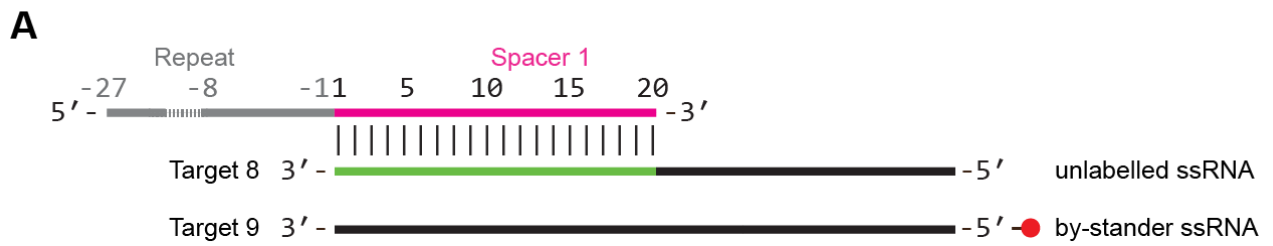


Fig. S12. *Sb*-gRAMP-crRNA1 has no collateral activity against non-complementary by-stander RNA. **(A)** Schematic of the collateral cleavage experiment involving unlabeled target RNA (Target 8) complementary to crRNA1 and Cy5-labeled non-complementary bystander RNA (Target 9). Substrate details are listed in table S5. **(B)** Denaturing urea PAGE gel of 200 nM *Sb*-gRAMP-crRNA1 incubated with 2-fold molar excess of Target 8 and 100 nM Target 9.

Cas7-#1 Cas11 Cas7-#2 Cas7-#3 Cas7-#4



	410	420	430	440	450	460	470	480
KHE91659.1	PPEGIETK	EWIIV	GRLLKAA	TPFFYFGV	QPS	DSIPGKEK	...KSE	SLVINEHT
NUN21993.1	PLGGV	.KEWII	GRLLKAB	TPFFYFGV	QSS	SFSDSTQDDLLDLPDIVNTD	EKLEANEQ	TSFRILMDKKG
GAB61731.1	PLGGV	.KEWII	GRLLKAB	TPFFYFGV	QSS	SFSDSTQDDLLDLPDIVNTD	EKLEANEQ	TSFRILMDKKG
KAA0249751.1	PLGGV	.KEWII	GRLLKAB	TPFFYFGV	QSS	SFSDSTQDDLLDLPDIVNTD	EKLEANEQ	TSFRILMDKKG
MBC6927464.1	PLGGV	.KEWII	GRLLKAB	TPFFYFGV	QSS	SFSDSTQDDLLDLPDIVNTD	EKLEANEQ	TSFRILMDKKG
WP_124327589.1	SIGSV	LKETIV	GELVAK	TPFFFGV	Q	DEDAK	...Q	TDLQVLLTPDN
OQY58162.1	GISV	.EKETI	MGTLKAB	TPFFFGV	Q	ESKEK	...Q	TDLMLLLDQGN
MBF0120744.1	FISSVPQY	ETIIQ	CKLIAK	TPFFFGV	Q	LENDET	...Q	SSYKLLLDNKN
MBF0452212.1	DIQIVPDR	EFIFY	GTLTSE	TPFFFGV	Q	LESEET	...Q	TDFTLLDRNN
MBF0451763.1	TKNSF	...WII	TGLESQ	TPFFFGV	Q	LESTGGN	...Q	TDIPTVDANG
KPA14974.1KWI	ISGELQAT	TPFFYIG	HVN	KTSHTRSTIFLNMNG
NPA15996.1	RRSFY	...EWIV	GRLLKAL	TPFFHGD	AS	EREGGILLTSDG

Cas7-#2

	490	500	510	520	530	540	550	560
KHE91659.1	TAFG	.SGCNVST	GQIIL	CNKVC	IEMR	ITLKS	VS	SD
NUN21993.1	TAFGGS	GCIVEL	GRMIP	CDCKVCA	IMRK	ITVMS	SRSE	.NIEL
GAB61731.1	TAFGGS	GCIVEL	GRMIP	CDCKVCA	IMRK	ITVMS	SRSE	.NIEL
KAA0249751.1	TAFGGS	GCIVEL	GRMIP	CDCKVCA	IMRK	ITVMS	SRSE	.NIEL
MBC6927464.1	TAFGGS	GCIVEL	GRMIP	CDCKVCA	IMRK	ITVMS	SRSE	.NIEL
WP_124327589.1	TYFD	.SPCNAEL	GGR	PCMKCT	CRIMRG	ITVMD	ARSE	.YNAP
OQY58162.1	SVLGT	.GCNAEV	GR	PCPCVCR	IMKN	ITVMD	TRSS	.TDIL
MBF0120744.1	NILGT	.GCNVEL	GGV	PCCKVCS	IMRN	ITVMD	SRSN	.YSEF
MBF0452212.1	I	VMDDI	GCDVRI	GGY	QCMPIC	IMRN	ITVMD	VRNE
MBF0451763.1	SMVSN	NCN	LVDI	GISR	PCVQ	TL	LSQ	CKFED
KPA14974.1	LVFG	.DSCNTP	VGSRV	.CYQV	QIMRC	IKFED	ALSD	.VDSF
NPA15996.1	WA	.GAVACE	VYK	GRKNL	CTCDV	CRIMR	RLIKD	CFSD

Cas7-#2

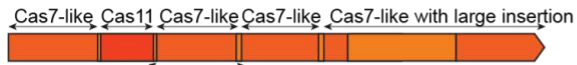
	570	580	590	600	610	620	630
KHE91659.1	...	K	FPEQ	LSS	VIRYWE	ENDGKN	GMAWL
NUN21993.1	...	DA	LPRE	LWS	VIRYWM	...	GMAWL
GAB61731.1	...	DA	LPRE	LWS	VIRYWM	...	GMAWL
KAA0249751.1	...	DA	LPRE	LWS	VIRYWM	...	GMAWL
MBC6927464.1	...	DA	LPRE	LWS	VIRYWM	...	GMAWL
WP_124327589.1	...	EDG	LPDAL	KTV	LKW	WAE	...
OQY58162.1	...	KT	LPKE	LRNV	LN	NWTE	...
MBF0120744.1	...	YKNP	DSEK	IPDS	LEK	VLT	WTE
MBF0452212.1	...	DT	GPPES	LIK	VLL	NWVA	...
MBF0451763.1	...	DIN	...	INED	LKKV	LG	WNS
KPA14974.1	...	NEI	MSQ	HYEV	LN	NWNTN	...
NPA15996.1	...	DRE	FPEE	LAV	V	LKW	WSE

Cas7-#2

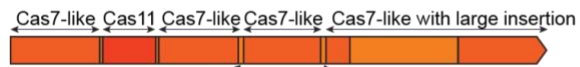
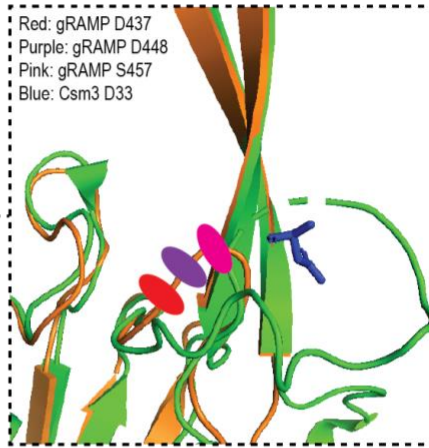
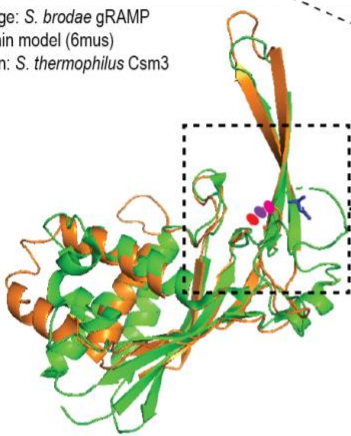
	640	650	660	670	680	690
KHE91659.1	M	...	GESSLP	DGLIP	YKFFEE	...
NUN21993.1	I	...	TEITN	LFKTE	EVKFFESYS	...
GAB61731.1	I	...	AEITN	LFKTE	EVKFFESYS	...
KAA0249751.1	I	...	AEITN	LFKTE	EVKFFESYS	...
MBC6927464.1	I	...	AEITN	LFKTE	EVKFFESYS	...
WP_124327589.1	L	...	EELK	RLNS
OQY58162.1	LEGGAG	GC	SFGLSD	PLK	GWHAED	LK
MBF0120744.1	DNLD	KLKFD	NL	PLK
MBF0452212.1	DL	ML	PLK	...
MBF0451763.1	YIGL	KKSE	V	DHL	IDDK	KNID
KPA14974.1	V	...	AD	...	PIK	WTL
NPA15996.1	C	KIEK	VSL

Cas7-#3

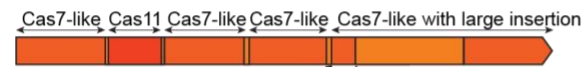
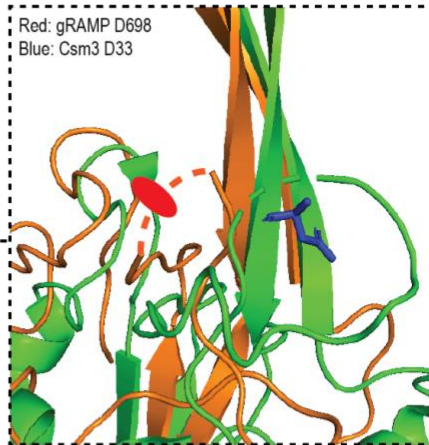
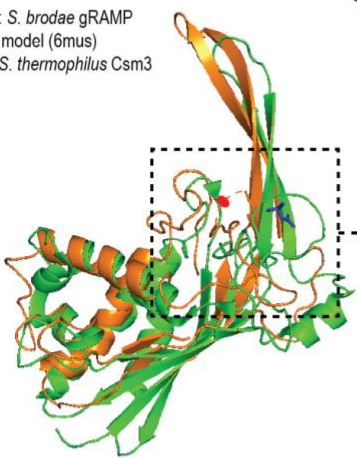
5 **Fig. S13.** gRAMP multiple sequence alignment of the suspected catalytic Cas7-like domains. Residues with identity are boxed and represented in different shades of red, with full conservation marked in dark red. Generated alanine substitutions are indicated with a dark blue asterisk and the aligning residues are marked with a blue box. Transparent orange blocks demarcate the Cas7-like domains. The alignment was generated using the Cobalt multiple alignment tool (41) with default settings and visualized using ESPript 3 (43).



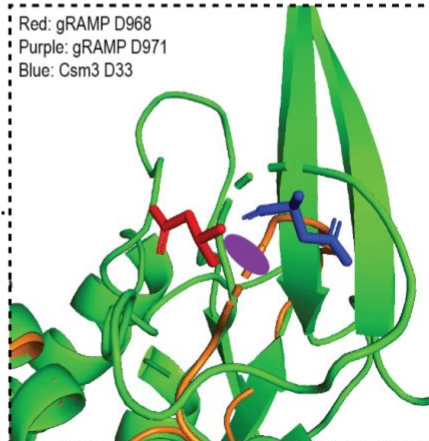
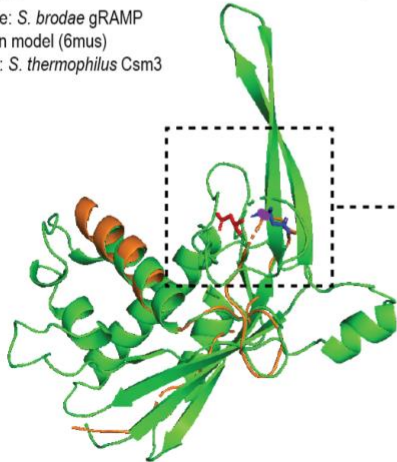
Orange: *S. brodae* gRAMP domain model (6mus)
Green: *S. thermophilus* Csm3



Orange: *S. brodae* gRAMP domain model (6mus)
Green: *S. thermophilus* Csm3



Orange: *S. brodae* gRAMP domain model (6mus)
Green: *S. thermophilus* Csm3



5 **Fig. S14.** Structural modelling of the Cas7-like domains. Models were generated using Phyre2 intensive mode (44) and aligned with the Csm3 structure of *Streptococcus thermophilus* (PDB: 6IG0) in PyMOL (45). The aspartic acid or serine residues (indicated with sticks or oval representation in red, purple and pink) of the Cas7-like domains in *Sb*-gRAMP that structurally aligned close to the active aspartic acid residue in *S. thermophilus* (indicated with sticks in blue) were subjected to alanine mutational analysis.

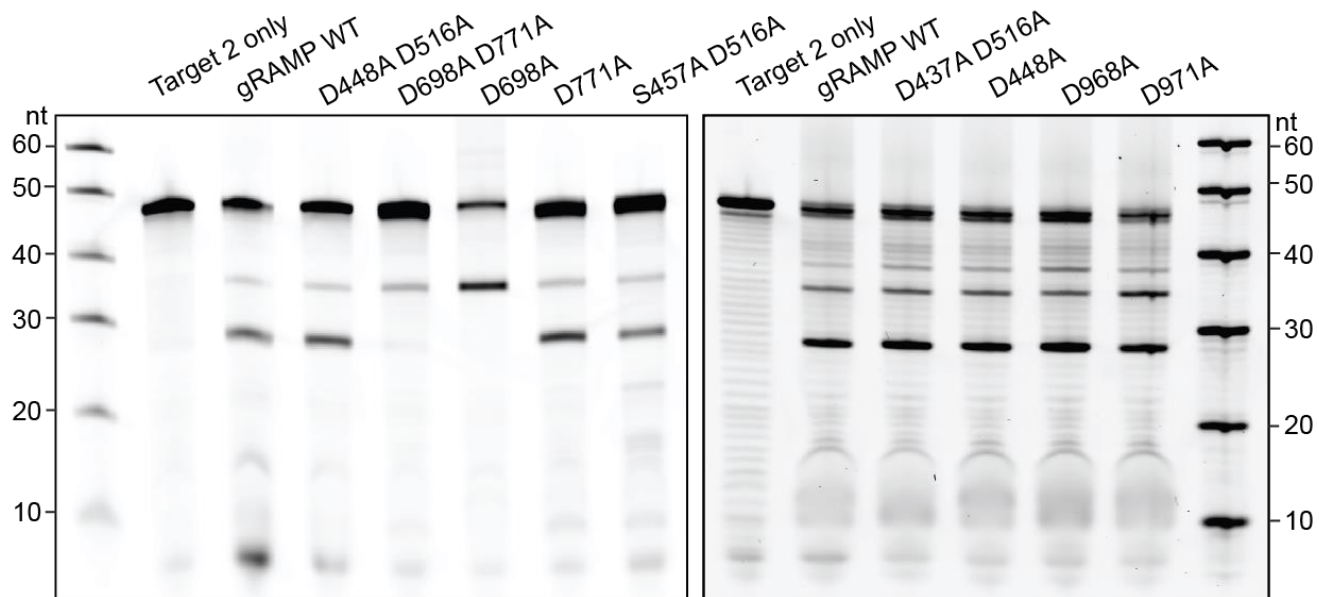


Fig. S15. *Sb*-gRAMP mutational analysis. Denaturing urea PAGE gel of target RNA cleavage reactions with crRNA1 loaded *Sb*-gRAMP mutants in which candidate active residues were mutated to alanines.

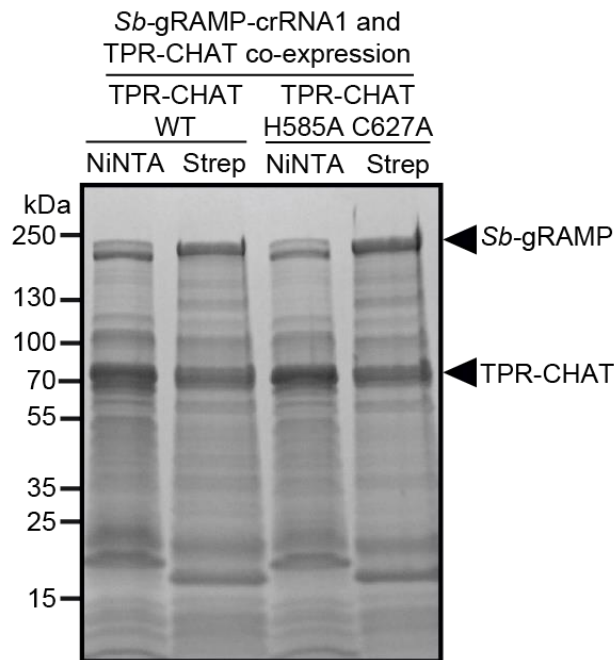
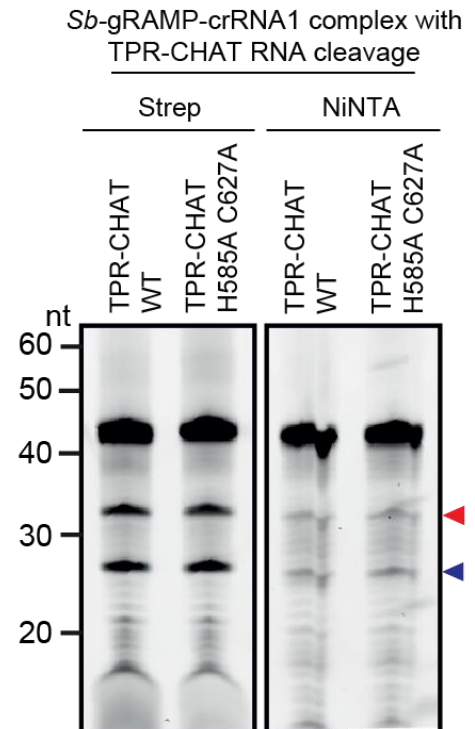
A**B**

Fig. S16. *Sb*-gRAMP-crRNA1 and TPR-CHAT co-expression. **(A)** Pulldown assays were performed using *Sb*-gRAMP-crRNA1 with wild-type TPR-CHAT or TPR-CHAT with inactivating mutations in the predicted protease domain (H585A and C627A), yielding similar band patterns and intensities in each condition. **(B)** The samples after pulldown were incubated with 100 nM target RNA cognate to crRNA1 (Target 2). Cleavage products are indicated with red and blue arrowheads.

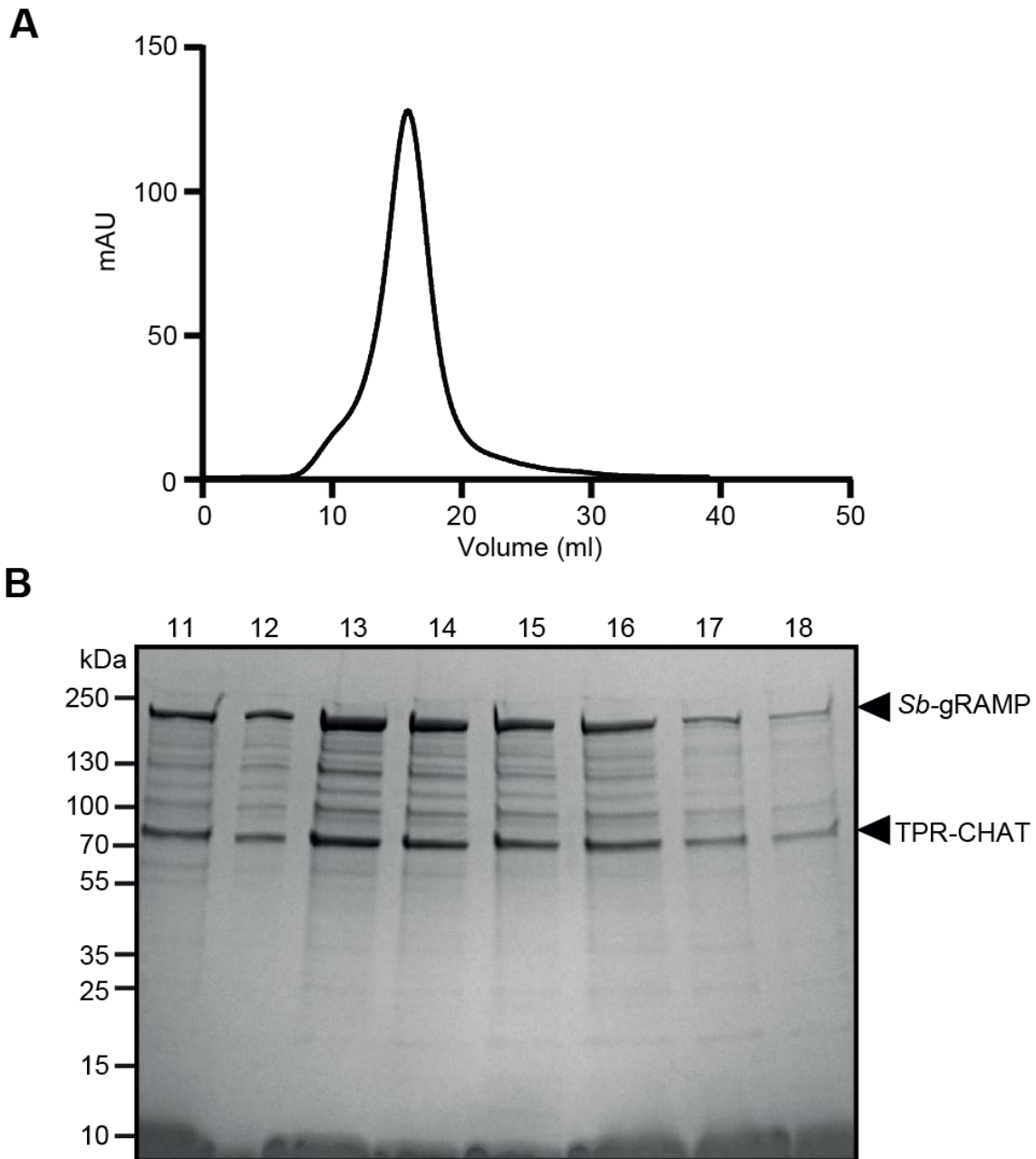


Fig. S17. Heparin purification of *Sb-gRAMP*-crRNA1 complexed with TPR-CHAT. **(A)** The UV₂₈₀ absorbance profile after elution of *Sb-gRAMP*-crRNA1 complexed with TPR-CHAT from the heparin column. **(B)** Heparin elution volumes corresponding to the peak analyzed with SDS-PAGE.

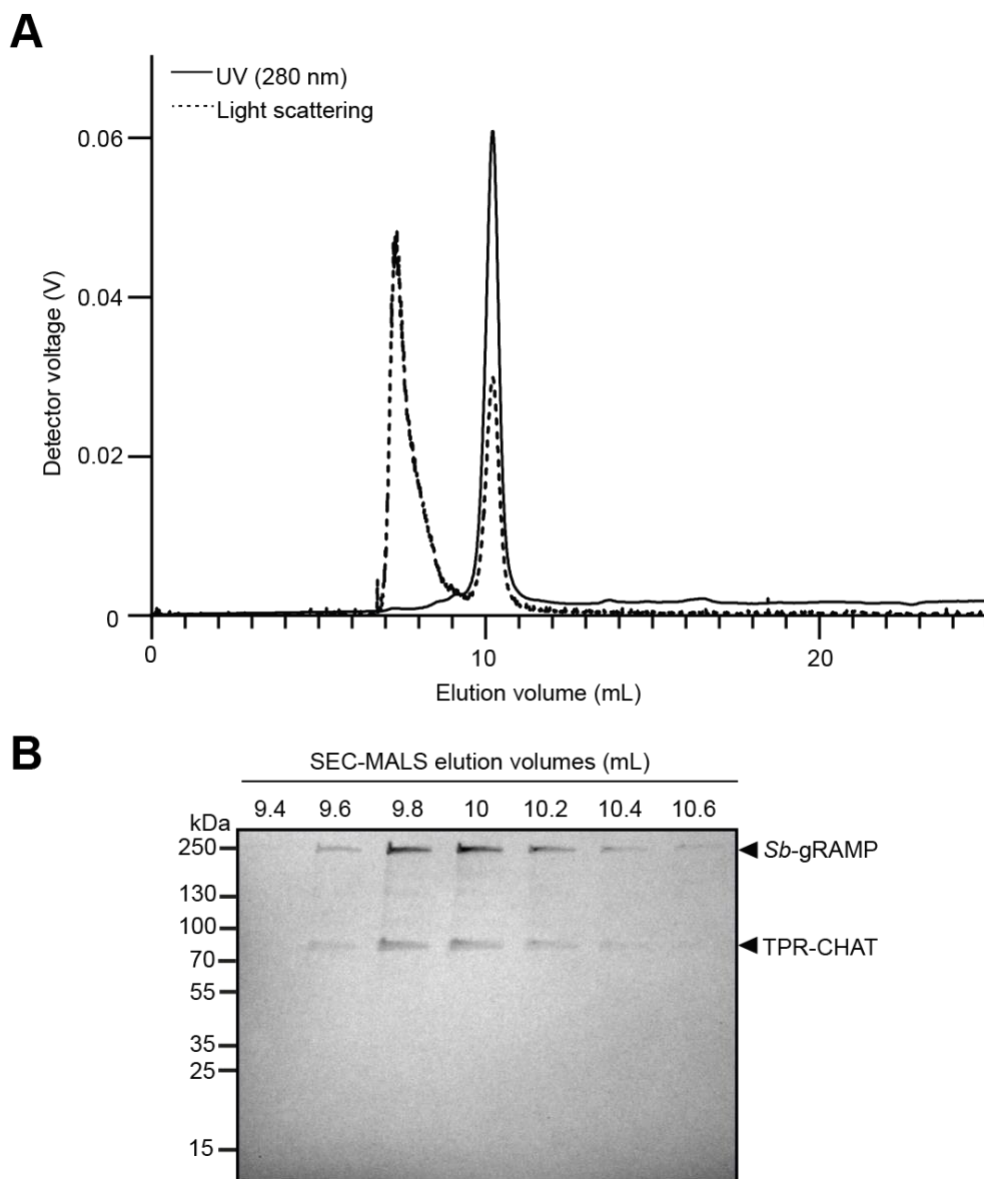


Fig. S18. SEC-MALS analysis of *Sb*-gRAMP-crRNA1 complexed with TPR-CHAT. **(A)** Complete SEC-MALS chromatogram showing the light scattering and UV₂₈₀ absorbance profiles for *Sb*-gRAMP-crRNA1 complexed with TPR-CHAT. **(B)** SDS-PAGE analysis of the collected SEC-MALS elution volumes.

5

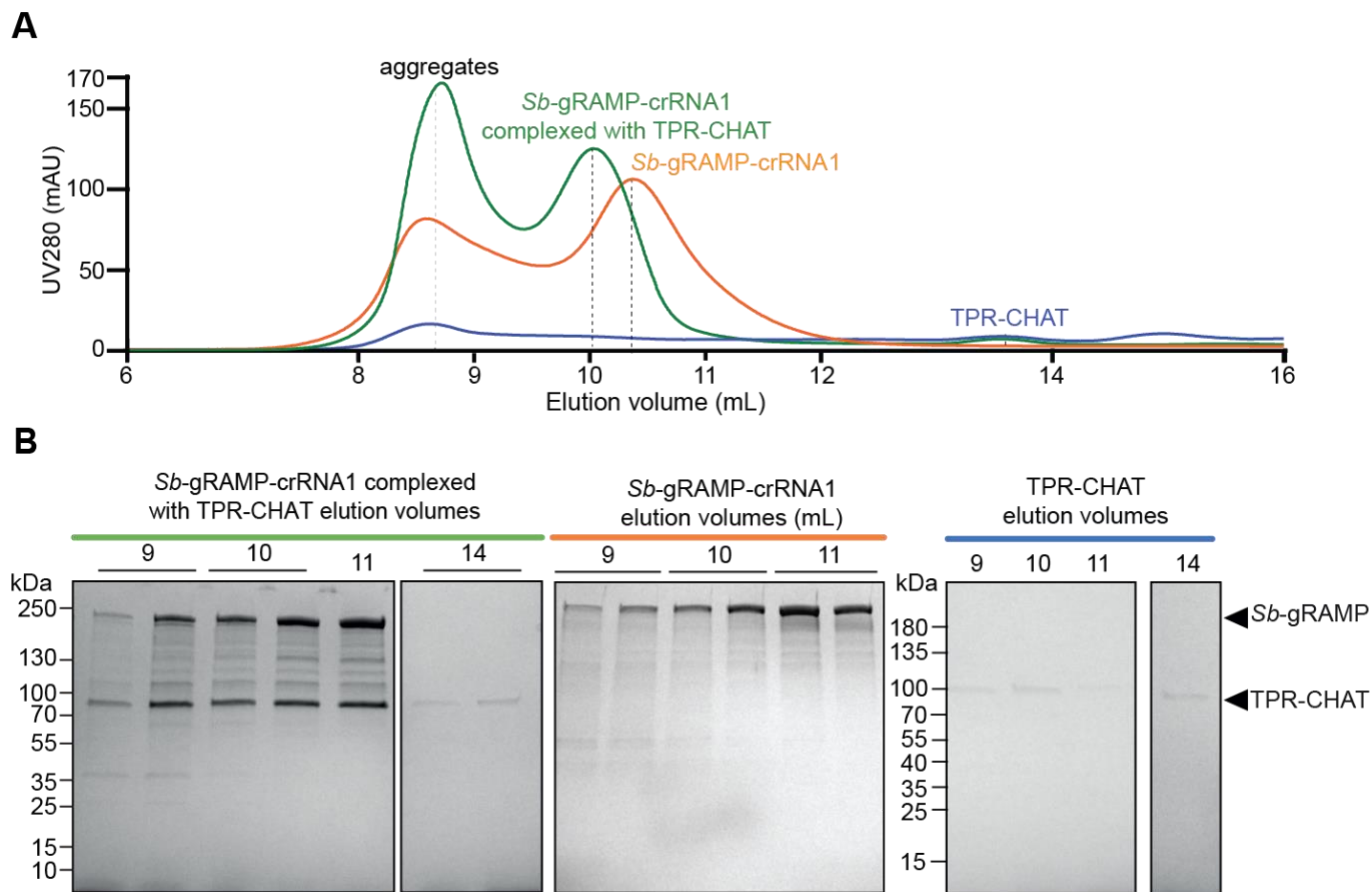


Fig. S19. Size-exclusion chromatography (SEC) of *Sb*-gRAMP-crRNA1, *Sb*-gRAMP-crRNA1 complexed with TPR-CHAT and TPR-CHAT alone. **(A)** Chromatograms showing the absorbance at 280 nm. **(B)** SDS-PAGE analysis of the elution volumes corresponding to the peaks.

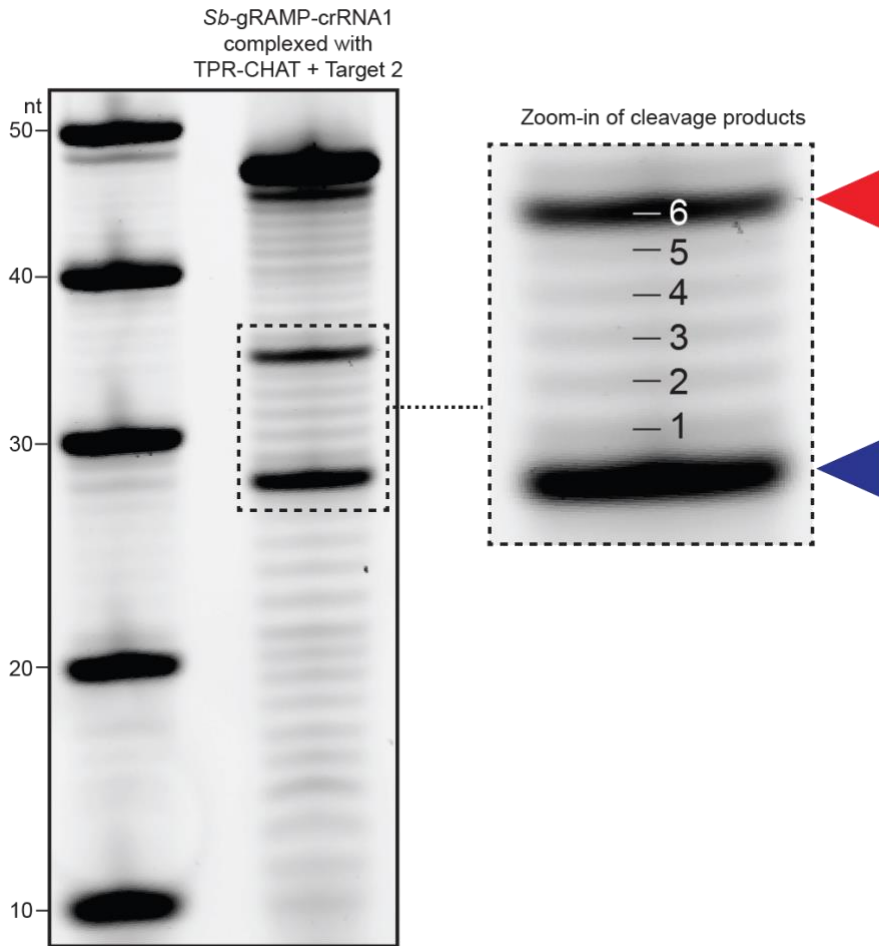


Fig. S20. The cleavage products generated by *Sb*-gRAMP-crRNA1 complexed with TPR-CHAT are 6 nt apart. Denaturing urea PAGE gel of a cleavage reaction of *Sb*-gRAMP-crRNA1 complexed with TPR-CHAT and cognate Target 2, with a zoom-in of the cleavage products (indicated with arrowheads) in which nucleotide counting steps are indicated.

5

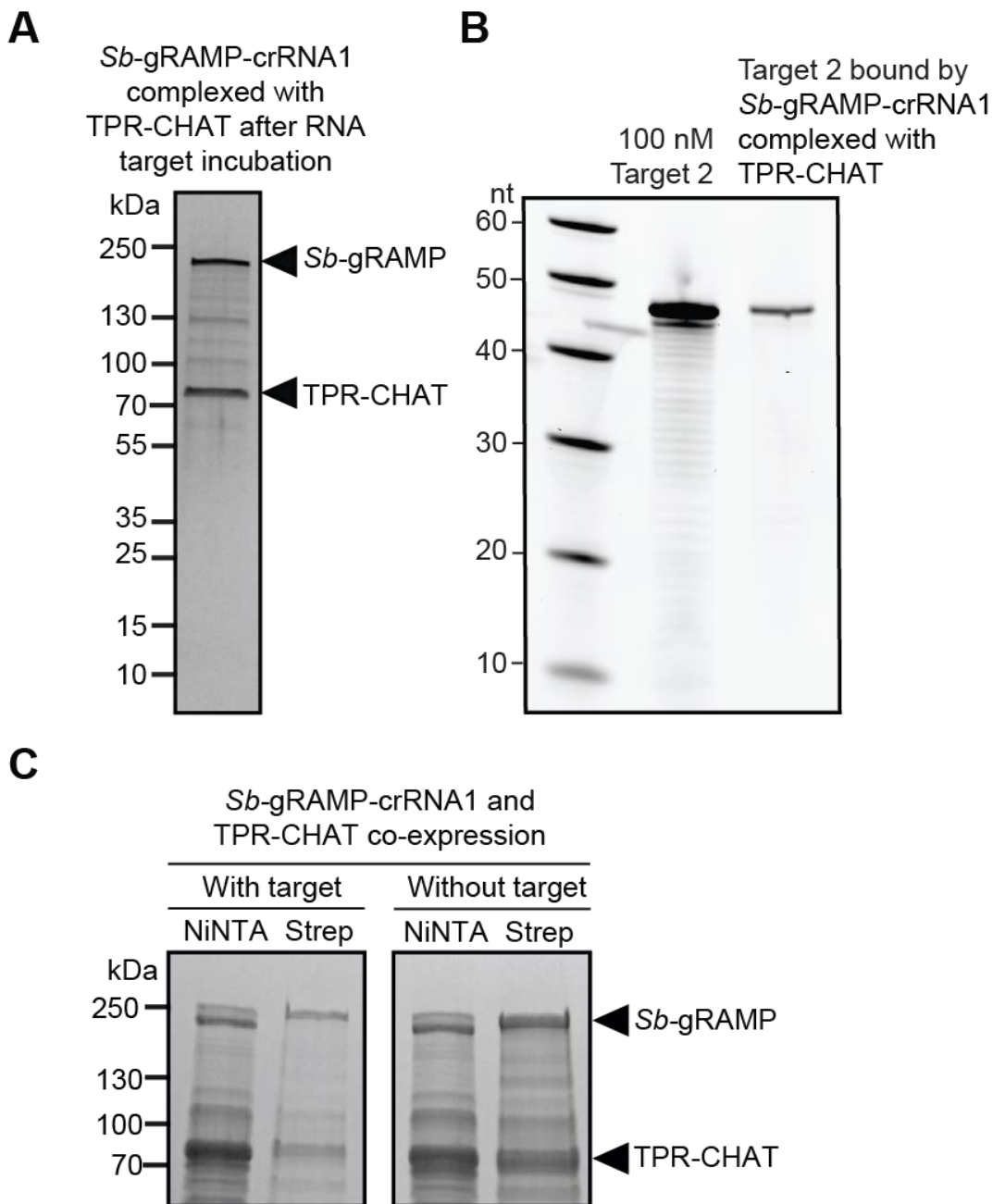


Fig. S21. TPR-CHAT remains complexed with *Sb*-gRAMP-crRNA1 upon target recognition. **(A)** SDS-PAGE analysis of SEC purified *Sb*-gRAMP-crRNA1 complexed with TPR-CHAT after incubation with cognate target RNA (Target 2) for 4 hours in the absence of MgCl₂. **(B)** RNA bound to SEC purified *Sb*-gRAMP-crRNA1 complexed with TPR-CHAT, indicating successful target binding. **(C)** SDS-PAGE analysis of *Sb*-gRAMP-crRNA1 complexed with TPR-CHAT overexpressed in the presence or absence of a target RNA.

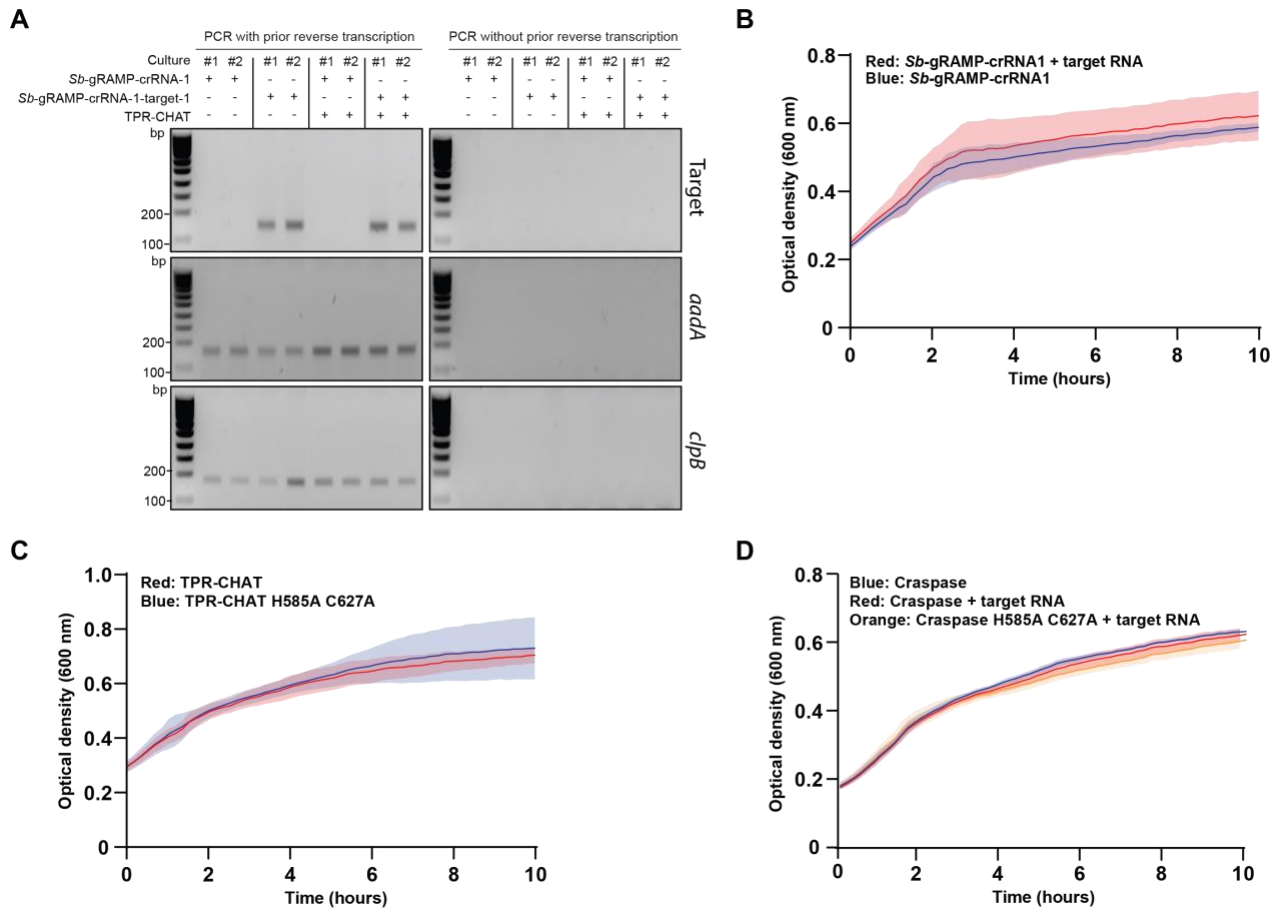


Fig. S22. Growth curves of *E. coli* during type III-E expression and target RNA production. (A) RT-PCR reactions of RNA extracted from induced cells to verify target RNA and control RNA production. Plasmid encoded spectinomycin resistance (aminoglycoside adenyltransferase; *aadA*) RNA or genome encoded caseinolytic peptidase B (*clpB*) were used as internal controls. Data represent biological duplicates. (B) OD₆₀₀ measurements of cells expressing only *Sb-gRAMP-crRNA1* (blue) or *Sb-gRAMP-crRNA1* in the presence of target RNA (red), (B) only TPR-CHAT (red) or TPR-CHAT H585A C627A (blue) and (C) Craspase or Craspase with TPR-CHAT H585A C627A in the presence (red, orange) and absence (blue) of target RNA. Data represent biological triplicates with standard deviation area bands filled.

Table S1. CRISPR-Cas type III-E spacer analysis. Listed are spacers from CRISPR-Cas type III-E loci with identified targets, the percentage of nucleotide identity, the target strand orientation, the source of the hit and whether the source of the hit was predicted to be of MGE origin.

Spacer	Target	Identity	Orientation	Source	MGE predicted
JAADEW010 000104.1	JAADEW 01000010 4.1	100%	Coding	Deferribacteres bacterium	No
NZ_CP06180 0.1_12:1	SDBT010 09396.1	91%	Coding	Marine sediment metagenome	No
NZ_CP06180 0.1_10:19	Ga021040 1_100116 68	90%	Coding	Forest soil metagenome	No
JRYO010001 85.1_1:6/1- 34	OVUK010 24005.1	94%	Coding	Aquaculture metagenome	No
NZ_BEXT01 000001.1_7:2 2/1-31	ERZ84053 7.224968- NODE- 224970	90%	Coding	Marine metagenome	No
JRYO010001 85.1_1:8/1- 37	JRYO010 00117	92%	Coding	Candidatus Scalindua brodae	Yes
MVRP01000 104.1_13:4/1 -48	MVRP010 00213.1	87%	Coding	Syntrophorhabdaceae bacterium PtaU1	No

MVRP01000 104.1_13:1/1 -47	MVRP010 00160.1	88%	Coding	Syntrophorhabdaceae bacterium PtaU1	No
JPDT010006 35.1_5:30	UYTZ010 00008.1	91%	Coding	human gut metagenome	No
JPDT010029 93.1_36:84	OFGZ010 02972.1	94%	Not determined	Mouse gut metagenome	No
JAABRU010 000211.1_1:8	LR796420	91%	Template	Phage	Yes
JPDT010029 93.1_36:91	LBBO010 04998.1	91%	Coding	Hydrothermal vent metagenome	No
JPDT010026 63.1_30:10	CEVW010 70774.1	94%	Template	Marine metagenome	No
JPDT010029 93.1_36:35	CESD010 17330.1	91%	Coding	Marine metagenome	No
JPDT010029 93.1_36:85	CERB012 84573.1	91%	Not determined	Marine metagenome	No
JPDT010006 35.1_5:6	BK043628	91%	Coding	Phage	Yes
ERZ650233. 69-NODE- 69_1:1	APMI011 13767.1	100%	Not determined	Wastewater metagenome	No
JPDT010029 93.1_36:11	AACY020 545844.1	91%	Coding	Marine metagenome	No

JPDT010026 63.1_30:10	LR796345	91%	Coding	Phage	Yes
JPDT010006 35.1_5:29	ERZ84101 0.367050- NODE- 367053	91%	Not determined	Marine metagenome	Yes

Table S2. DNA sequences of the spacers and repeat in the *Candidatus* “*Scalindua brodae*” CRISPR array.

Spacer	DNA sequence (5' → 3')	Length (nt)
1	CCAATTTTCTGCCCCGGACTCCACGGCTGTTACTAGAG	38
2	AGTTTCCTGTTTTTTTTGCTCCCTAACGCTACTTTGAAT	39
3	AATTATCATTGGACAGCTTCCCTCATTATTTGAGGTC	39
4	GAAAAAAAAAAGTAAAGTTCAGGGGCAAGTGCCAAA	37
5	CCCTTTGCTTCTTCTCTAGTGTTTCTATCCATGTTTGT	38
6	TTACGAAGTATCTCCGTACGAACCTTTTCACTGT	34
7	AGAATTGGTATTATTTTTCCAGTGTAATAATACC	35
8	ACCATTTTGTTCATTATTTATTGTCATGTTAGAAA	35
9	TCTTCAGCAATTACTTCTTTACGAAGAGATAACTTT	36
10	AAAATCTCAAGCCTCAAGCATATACTCAAATCATT	37
11	ATCATTACCATCCATATGTTCTGATGACTGTCTCTGCTGTA	41
Repeat	GTTATGAAACAAGAGAAGGACTTAATGTCACGGTAC	36

Table S3. The experimentally calculated versus theoretic molar mass for *Sb*-gRAMP-crRNA and *Sb*-gRAMP-crRNA1 complexed with TPR-CHAT. For the theoretical molar mass of the RNA, 55 nt ssRNA of crRNA1 (AAACAAGAGAAGGACUUAUGUCACGGUACCCAAUUUCUGC CCCGGACUCCACG) with 5' phosphate was used and calculated using MolBioTools DNA calculator (www.molbiotools.com). The molar mass of TPR-CHAT is 83.8 kDa.

5

	Experimentally calculated (<i>theoretical</i>) total molar mass (kDa)	Experimentally calculated (<i>theoretical</i>) protein molar mass (kDa)	Experimentally calculated (<i>theoretical</i>) RNA molar mass (kDa)
<i>Sb</i>-gRAMP-crRNA1	242.5 ± 2.4 (231.7)	225.7 ± 2.3 (214.0)	16.8 ± 2.3 (17.7)
<i>Sb</i>-gRAMP-crRNA3	241.9 ± 0.5 (231.7)	224.7 ± 0.5 (214.0)	17.2 ± 0.5 (17.7)
<i>Sb</i>-gRAMP-crRNA1 complexed with TPR-CHAT	315.4 ± 2.8 (315.5)	301.6 ± 2.7 (297.8)	13.8 ± 3.0 (17.7)

Table S4. Mass spectrometry analysis of two in-gel digestion samples of *Sb*-gRAMP complexed with TPR-CHAT. Sample derived from in-gel digestion of upper gel band (~214 kDa) or lower gel band (~83 kDa) in fig. S19B, elution 11.

Number of unique peptide per protein	Number of spectra	Average mass (Da)	Description	-10 log P	Gel band (fig. S19B, elution 11)
251	838	214,018	<i>Sb</i> -gRAMP	611.04	Upper
5	5	83,785	TPR-CHAT	106.64	Upper
3	3	88,946	Bifunctional aspartokinase/homoserine dehydrogenase OS=Escherichia coli (strain B / BL21-DE3) OX=469008 GN=ECBD_4083 PE=3 SV=1	67.33	Upper
89	315	83,785	TPR-CHAT	406.92	Lower
117	175	214,018	<i>Sb</i> -gRAMP	366.34	Lower
18	23	69,115	Chaperone protein DnaK OS=Escherichia coli (strain B / BL21-DE3) OX=469008 GN=dnaK PE=2 SV=1	218.39	Lower
17	22	61,158	30S ribosomal protein S1 OS=Escherichia coli (strain B / BL21-DE3) OX=469008 GN=ECBD_2684 PE=3 SV=1	215.08	Lower
8	8	77,101	Polyribonucleotide nucleotidyltransferase OS=Escherichia coli (strain B / BL21-DE3) OX=469008 GN=pnp PE=3 SV=1	140.38	Lower

4	5	28,744	4-hydroxy-tetrahydrodipicolinate reductase OS=Escherichia coli (strain B / BL21-DE3) OX=469008 GN=dapB PE=3 SV=1	121.47	Lower
4	4	48,532	Aspartokinase OS=Escherichia coli (strain B / BL21-DE3) OX=469008 GN=ECBD_4013 PE=3 SV=1	102.67	Lower
4	4	66,096	Acetyltransferase component of pyruvate dehydrogenase complex OS=Escherichia coli (strain B / BL21-DE3) OX=469008 GN=ECBD_3504 PE=3 SV=1	101.65	Lower
2	2	57,329	60 kDa chaperonin OS=Escherichia coli (strain B / BL21-DE3) OX=469008 GN=groL PE=3 SV=1	53.17	Lower

Table S5. Substrates used for in vitro cleavage experiments.

Name	Sequence (5'→3')	Length (nt)	Side Cy5-label	Description	Vendor
Target 1	CUCUAGU AACAG CCGUGGAGUCCG GGGCAGAAAAU GG	38	5'	ssRNA complementary to crRNA1	IDT
Target 2	CUCUAGU AACAG CCGUGGAGUCCG GGGCAGAAAAU GGACGAUUAA	46	5'	ssRNA complementary to crRNA1 with non-matching PFS	IDT
Target 3	CUCUAGU AACAG CCGUGGAGUCCG GGGCAGAAAAU GGACGAUUAA CU	48	3'	ssRNA complementary to crRNA1	IDT
Target 4	CUCUAGU AACAG CCGUGGAGUCCG GGGCAGAAAAU GGGUACCGUG	46	5'	ssRNA complementary to crRNA1 with matching PFS	IDT
Target 5	CTCTAGT AACAGC CGTGGAGTCCGGG GCAGAAAATTGGA CGATTAA	46	5'	ssDNA complementary to crRNA1	IDT
Target 6	GACCUCG AAAUA AUGAGGGAAGCU GUCCAAAUGAUA AUU	39	5'	ssRNA non- complementary to crRNA1	Horizon discovery
Target 7	GACCUCG AAAUA AUGAGGGAAGCU GUCCAAAUGAUA AUU	39	5'	ssRNA complementary to crRNA3	Horizon discovery

Target 8	CUCUAGU AACAG CCGUGGAGUCCG GGGCAGAAA AU GG	38	None	Unlabelled ssRNA complementary to crRNA1	IDT
Ladder 10 nt	UCGGAUUCUG	10	5'	Used as RNA ladder in cleavage experiments	IDT
Ladder 20 nt	GCGGAUUCUGAA ACGGUGGA	20	5'	Used as RNA ladder in cleavage experiments	IDT
Ladder 30 nt	CAAAGUGC UUAC AGUGCAGGUAGU GAUAUG	30	5'	Used as RNA ladder in cleavage experiments	IDT
Ladder 40 nt / Target 9	UUUUUUUUUUUC CGCGGCUUUUUU UUUUUUUUUCCG CGGC	40	5'	Used as RNA ladder in cleavage experiments and as by-stander RNA in collateral activity assay	IDT
Ladder 50 nt	GUCAUAGGAGAA GUAUUAACAUCU ACAGGGAGUCUA UAUUGAGGUACU AG	50	5'	Used as RNA ladder in cleavage experiments	IDT
Ladder 60 nt	GUCAUAGGAGAA GUAUUAACAUCU ACAGGGAGUCUA UAUUGAGGUACU AGUCGGAUUCUG	60	5'	Used as RNA ladder in cleavage experiments	IDT
dNMPpos28 (dNMP underlined)	CUCUAGU AACAG CCGUGGAGUCCG GGGCAGAAA AU GG	38	5'	Used as auto- hydrolysis internal control ladder	IDT

dNMPpos34 (dNMP underlined)	CUCUAGU AACAG CCGUGGAGUCCG GGCAGAAA <u>A</u> UU GG	38	5'	Used as auto- hydrolysis internal control ladder	IDT
-----------------------------------	-------------------------------------------------------------	----	----	-----------------------------------------------------------	-----

Table S6. Plasmids used in this study.

Plasmid	Description	Name in paper	Antibiotic resistance marker
pTU387	pACYC Duet-1 containing full Type III-E system <i>Candidatus</i> “ <i>Scalindua brodae</i> ” CRISPR array	pCRISPR-WT	Chloramphenicol
pTU398	13S-S <i>Candidatus</i> “ <i>Scalindua brodae</i> ” Twin-Strep SUMO tagged RAMP (codon optimization)	pGRAMP	Spectinomycin
pTU400	pACYC Duet-1 containing <i>Candidatus</i> “ <i>Scalindua brodae</i> ” CRISPR array spacer 1 (five times)	pCRISPR-1	Chloramphenicol
pTU408	13S-S <i>Candidatus</i> “ <i>Scalindua brodae</i> ” Twin-Strep SUMO tagged RAMP S457A (codon optimization)	pGRAMP S457A	Spectinomycin
pTU410	13S-S <i>Candidatus</i> “ <i>Scalindua brodae</i> ” Twin-Strep SUMO tagged RAMP D516A (codon optimization)	pGRAMP D516A	Spectinomycin
pTU414	13S-S <i>Candidatus</i> “ <i>Scalindua brodae</i> ” Twin-Strep SUMO tagged RAMP D437A D516A (codon optimization)	pGRAMP D437A D516A	Spectinomycin
pTU415	13S-S <i>Candidatus</i> “ <i>Scalindua brodae</i> ” Twin-Strep SUMO tagged RAMP D448A (codon optimization)	pGRAMP D448A	Spectinomycin
pTU416	13S-S <i>Candidatus</i> “ <i>Scalindua brodae</i> ” Twin-Strep SUMO tagged RAMP D448A D516A (codon optimization)	pGRAMP D448A D516A	Spectinomycin
pTU417	13S-S <i>Candidatus</i> “ <i>Scalindua brodae</i> ” Twin-Strep SUMO tagged RAMP D698A (codon optimization)	pGRAMP D698A	Spectinomycin
pTU418	13S-S <i>Candidatus</i> “ <i>Scalindua brodae</i> ” Twin-Strep SUMO tagged RAMP D771A (codon optimization)	pGRAMP D771A	Spectinomycin

pTU419	13S-S <i>Candidatus</i> “Scalindua brodae” Twin-Strep SUMO tagged RAMP D698A D771A (codon optimization)	pGRAMP D698A D771A	Spectinomycin
pTU420	13S-S <i>Candidatus</i> “Scalindua brodae” Twin-Strep SUMO tagged RAMP D698A (codon optimization)	pGRAMP D968A	Spectinomycin
pTU421	13S-S <i>Candidatus</i> “Scalindua brodae” Twin-Strep SUMO tagged RAMP D971A (codon optimization)	pGRAMP D971A	Spectinomycin
pTU422	13S-S <i>Candidatus</i> “Scalindua brodae” Twin-Strep SUMO tagged RAMP (codon optimization) enriched with CRISPR array spacer 1 (five times)	pGRAMP-CRISPR-1	Spectinomycin
pTU423	13S-S <i>Candidatus</i> “Scalindua brodae” Twin-Strep SUMO tagged RAMP (codon optimization) enriched with CRISPR array spacer 1 (five times) and DNA encoding for RNA target 1 (5'-CUCUAGU AACAGCCGUGGAGUCCGGG GCAGAAA AUUGG-3', which is complementary to spacer 1)	pGRAMP-CRISPR-1-target-1	Spectinomycin
pTU424	pACYC containing <i>Candidatus</i> “Scalindua brodae” TPR-CHAT (codon-optimized)	pTPR-CHAT	Chloramphenicol
pTU425	pACYC containing <i>Candidatus</i> “Scalindua brodae” TPR-CHAT H585A C627A (codon-optimized)	pTPR-CHAT H585A C627A	Chloramphenicol
pTU426	13S-S containing DNA encoding for RNA target 1 (5'-CUCUAGU AACAGCCGUGGAGUCCGGG GCAGAAA AUUGG-3', which is complementary to spacer 1)	pTarget	Spectinomycin
pTU433	pACYC Duet-1 containing <i>Candidatus</i> “Scalindua brodae” CRISPR array spacer 3 (five times)	pCRISPR-3	Chloramphenicol

Table S7. Primers used in this study. “P” represents 5'-phosphorylation of the primer.

Name	Sequence (5'→3')	Description (Forward/Reverse couples)
BN2780	TGCATTGGATTGGAAGTACAG GTTTCCTCGATC	On 13S-S for pGRAMP construction
BN2781	TAATAACATTGGAAGTGGATA ACGGATCCGCGATC	On 13S-S for pGRAMP construction
BN2782	GATCGAGGAAAACCTGTACTT CCAATCCAATGCAATGAAAA GCAACGACATGAAC	On codon-optimized <i>Sb</i> -gRAMP fragment
BN2783	GATCGCGGATCCGTTATCCAC TTCCAATGTTATTATTACACC ATTTTACCATCACGTTTC	On codon-optimized <i>Sb</i> -gRAMP fragment
BN2289	GATATCCAATTGAGATCTGCC ATATGTATATCTCCTTCTTATA C	On pACYC Duet-1 for pCRISPR-WT construction
BN2290	GATCGCTGACGTCGGTACCCT CGAGTC	On pACYC Duet-1 for pCRISPR-WT construction
BN2291	CATATGGCAGATCTCAATTGG ATATCCAGACAAACGGTTTGC GAAGAAATAC	On <i>Candidatus</i> “ <i>Scalindua brodae</i> ” genomic DNA to obtain the wild-type CRISPR array
BN2292	GAGGGTACCGACGTCAGCGA TCTTCAATCAAACCTAAGTAC TTCTCTTG	On <i>Candidatus</i> “ <i>Scalindua brodae</i> ” genomic DNA to obtain the wild-type CRISPR array
BN3223	TATGTCTATTGCTGGGAGGTT TCAGCAAAAACCCCTC	On pCRISPR-1 to obtain CRISPR array to clone in pGRAMP-CRISPR-1
BN3228	CAATAAACCGGTAAATAATC GTATTGTACACGGCCG	On pCRISPR-1 to obtain CRISPR array to clone in pGRAMP-CRISPR-1

BN3225	TTTTGCTGAAACCTCCCAGCA ATAGACATAAGCGGC	On pGRAMP to construct pGRAMP- CRISPR-1
BN3226	TGTACAATACGATTATTTACC GGTTTATTGACTACCGGAAG	On pGRAMP to construct pGRAMP- CRISPR-1
BN2340	P- TTTTCCAATTTTCTGCCCCGG ACTCCACGGCTGTTACTAGAG ATTATTTCTAGAACTCG	On 13S-S to construct pTarget
BN2341	P- AATATTGGAAGTGGATAACG	On 13S-S to construct pTarget
BN3223	TATGTCTATTGCTGGGAGGTT TCAGCAAAAACCCCTC	On pTarget to construct pGRAMP-CRISPR- 1-target-1
BN3224	TGAGAAGCACACGGTGGAAA TTAATACGACTCACTATAGG	On pTarget to construct pGRAMP-CRISPR- 1-target-1
BN3227	GTCGTATTAATTTCCACCGTG TGCTTCTCAAATGC	On pGRAMP-CRISPR-1 to construct pGRAMP-CRISPR-1-target-1
BN3225	TTTTGCTGAAACCTCCCAGCA ATAGACATAAGCGGC	On pGRAMP-CRISPR-1 to construct pGRAMP-CRISPR-1-target-1
BN3151	TTTCTACAGGGGAATTGTTAT CC	On p2AT to construct pTPR-CHAT
BN3152	TACTAGCGCAGCTTAATTAAC C	On p2AT to construct pTPR-CHAT
BN3229	ACACAGAATGGTCAGCAGAC GC	On pTPR-CHAT to insert gBlock for pTPR- CHAT H585A C627A construction
BN3230	GAAACCGATCTGGTTCGCC	On pTPR-CHAT to insert gBlock for pTPR- CHAT H585A C627A construction

BN2987	CTGCCAGAGTTCACATAAACA GACGC	On pGRAMP together with mutant specific primer
BN2988	GGAAAAGCGTCTGTTTATGTG AACTCTGGC	On pGRAMP together with mutant specific primer
BN3065	AATGAACACACCGCCTTTAAC ATCCTGC	On pGRAMP to create S457A (with BN2988)
BN3066	GGATGTTAAAGGCGGTGTGTT CATTGATGACC	On pGRAMP to create S457A (with BN2987)
BN3063	CGCTAACGCTAGCTTTCAGTG TGATGC	On pGRAMP to create D516A (with BN2987)
BN3064	GCATCACACTGAAAGCTAGC GTTAGCG	On pGRAMP to create D516A (with BN2988)
BN3322	CGGAATGCTCGCACTCGGCTG C	On pGRAMP D516A to create pGRAMP D437A D516A (with BN2987)
BN3323	CAGCCGAGTGCGAGCATTCCG GG	On pGRAMP D516A to create pGRAMP D437A D516A (with BN2988)
BN3324	GAGAAAAAATCAGAAGCTAG CCTGGTCATC	On pGRAMP D516A to create pGRAMP D448A D516A (with BN2988)
BN3325	CATTGATGACCAGGCTAGCTT CTGATTTTTTC	On pGRAMP D516A to create pGRAMP D448A D516A (with BN2987)
BN3324	GAGAAAAAATCAGAAGCTAG CCTGGTCATC	On pGRAMP to create pGRAMP D448A (with BN2988)
BN3325	CATTGATGACCAGGCTAGCTT CTGATTTTTTC	On pGRAMP D516A to create pGRAMP D448A (with BN2987)

BN2985	TTGTAGGCAATTGCAGCACGA TTACCC	On pGRAMP to create pGRAMP D698A (with BN2987)
BN2986	CCGGGTAATCGTGCTGCAATT GCCTAC	On pGRAMP to create pGRAMP D698A (with BN2988)
BN2989	TTCGTTTTGAAGCTCTGGAAC TGATCAACG	On pGRAMP to create pGRAMP D771A (with BN2988)
BN2990	ATCAGTTCCAGAGCTTCAAAA CGAATTTTGC	On pGRAMP to create pGRAMP D771A (with BN2987)
BN2989	TTCGTTTTGAAGCTCTGGAAC TGATCAACG	On pGRAMP D698A to create pGRAMP D698A D771A (with BN2988)
BN2990	ATCAGTTCCAGAGCTTCAAAA CGAATTTTGC	On pGRAMP D698A to create pGRAMP D698A D771A (with BN2987)
BN3436	GATTATTCGGCAACCAGTGA TG	On pGRAMP to create pGRAMP D968A (with BN2988)
BN3437	TTCATCACTGGTTGCCGGAAT AATC	On pGRAMP to create pGRAMP D968A (BN2987)
BN3438	CGGATAACCAGTGCGGAAAAT GGTCTG	On pGRAMP to create pGRAMP D971A (with BN2988)
BN3439	TTTCAGACCATTTTCCGCACT GGTATCCG	On pGRAMP to create pGRAMP D971A (with BN2987)
BN3596	TAGTAACAGCCGTGGAGTCC	On pGRAMP-crRNA-1-target-1 to amplify target RNA
BN3599	TTTCGGGCTTTGTTAGCAGC	On pGRAMP-crRNA-1-target-1 to amplify target RNA
BN3596	TTTCGGGCTTTGTTAGCAGC	For amplification of target RNA cognate to crRNA1

BN3599	TAGTAACAGCCGTGGAGTCC	For amplification of target RNA cognate to crRNA1
BN3642	CAAGAATGTCATTGCGCTGC	For amplification of spectinomycin resistance (aminoglycoside adenylyltransferase; <i>aadA</i>) RNA
BN3643	TTTGAAACTTCGGCTTCCC	For amplification of spectinomycin resistance (aminoglycoside adenylyltransferase; <i>aadA</i>) RNA
BN3649	TACGACGATCGAGTCGGTCG	For amplification of caseinolytic peptidase (<i>clpB</i>) RNA
BN3650	GACCCGGCAATTGTTGCAGC	For amplification of caseinolytic peptidase (<i>clpB</i>) RNA

Table S8. Sequences used in this study.

Name	Sequence (5'→3')
Codon-optimized <i>Sb</i> -gRAMP	ATGAAAAGCAACGACATGAACATTACCGTGGAAGTACCTTTTTTTGA ACCGTATCGTCTGGTTGAATGGTTTGGATTGGGATGCACGTAAAAAAA GCCATAGCGCAATGCGTGGTCAGGCATTTGCACAGTGGACCTGGAAA GGTAAGGTCGTACCGCAGGTAAAAGCTTTATTACCGGTACACTGGT TCGTAGCGCAGTTATTAAGCAGTTGAAGAAGTCTGAGCCTGAATA ATGGTAAATGGGAAGGTGTTCCGTGTTGCAATGGTAGCTTTCAGACC GATGAAAGCAAAGGTAAAAAACCGAGCTTCTGCGTAAACGTCATAC CCTGCAGTGGCAGGCAAATAACAAAAACATTTGCGATAAAGAAGAG GCCTGTCCGTTTTGTATTCTGCTGGGTCGTTTTGATAATGCCGGTAAA GTGCATGAACGCAACAAAGATTATGATATCCACTTCAGCAACTTCGA CCTGGATCACAAACAAGAAAAAATGATCTGCGCCTGGTTGATATTG CAAGCGGTCGTATTCTGAATCGTGTGATTTTGATAACCGGCAAAGCCA AAGATTACTTTCGTACCTGGGAAGCAGATTATGAAACCTATGGCACC TATACCGGTTCGATTACCCTGCGTAATGAACATGCAAAAAAACTGCT GCTGGCAAGCCTGGGTTTTGTTGATAAACTGTGTGGTGCCTGTGTGC TATTGAGGTTATCAAAAAAAGCGAAAGTCCGCTGCCGAGCGATACCA AAGAACAGAGCTATACAAAAGATGATACCGTTGAAGTCTGAGCGAA GATCATAATGATGAACTGCGCAAACAGGCCGAAGTTATTGTTGAAGC ATTTAAGCAGAACGATAAACTGGAAAAAATTCGCATTCTGGCAGATG CAATTCGTACCCTGCGCCTGCATGGTGAAGGTGTGATTGAAAAAGAT GAGCTGCCGGATGGTAAAGAAGAACGCGATAAAGGTCATCATCTGTG GGATATTAAGTTCAGGGCACCGCACTGCGTACCAAACCTGAAAGAAC TGTGGCAGAGCAATAAAGATATTGGCTGGCGCAAATTTACCGAAATG CTGGGTAGCAATCTGTACCTGATCTATAAGAAAGAAACCGGTGGTGT TAGCACCCGTTTTTCGCATCCTGGGTGATACCGAGTATTATAGCAAAGC ACATGATAGCGAAGGTAGCGACCTGTTTATTCCGGTTACACCGCCTG AAGGTATTGAAACCAAAGAATGGATTATTGTGGGTTCGCTGAAAGCA GCAACCCCGTTTTATTTTCGGTGTTCAGCAGCCGAGTGATAGCATTCCG GGTAAGAGAAAAAATCAGAAGATAGCCTGGTCATCAATGAACACA CCAGCTTTAACATCCTGCTGGATAAAGAAAAATCGTTATCGTATTCCGC GTAGTGCCTGCGTGGTGCCCTGCGTCGCGATCTGCGTACCGCATTG GTAGCGGTTGTAATGTTAGCTTAGGTGGTCAGATTCTGTGCAATTGTA AAGTGTGTATTGAAATGCGTCGCATCACACTGAAAGATAGCGTTAGC GATTTTTTCAGAACCTCCGGAAATTCGCTATCGCATTGCAAAAAAATCCG GGTACAGCAACCGTGGAAGATGGTAGTCTGTTTGATATTGAAGTTGG TCCGGAAGGCCTGACCTTTCCGTTTGTCTGCGTTATCGTGGTCATAA ATTTCCAGAACAGCTGAGCAGCGTTATTTCGTTATTGGGAAGAAAATG ATGGCAAAAATGGTATGGCATGGTTAGGTGGCCTGGATAGCACCGGT AAAGGCCGTTTTGCCCTGAAAGACATTAATAATCTTTGAGTGGGATCT GAACCAGAAAATCAACGAATATATCAAAGAACGCGGTATGCGTGGC AAAGAAAAAGAATTACTGGAATGGGTGAAAGCAGTCTGCCTGATG GTCTGATTCCGTATAAATCTTTGAAGAACGTGAATGCCTGTTCCGT ACAAAGAAAACCTGAAACCGCAGTGGTCAGAAGTTCAGTATACCATT

GAAGTGGGTTACCGCTGCTGACCGCAGATACCATTAGCGCACTGAC
CGAACCGGGTAATCGTGATGCAATTGCCTACAAAAACGCGTGTATA
ACGATGGCAATAATGCCATTGAACCGGAACCGCGTTTTGCAGTAAA
AGTGAAACCCATCGTGGTATTTTTCGCACCGCAGTTGGTCGTCTACC
GGTGATCTGGGCAAAGAAGATCACGAAGATTGTACCTGTGATATGTG
CATTATCTTTGGCAATGAGCATGAGAGCAGCAAAATTCGTTTTGAAG
ATCTGGAACCTGATCAACGGCAACGAATTTGAAAAGCTGGAAAAACAT
ATTGACCACGTGGCCATTGATCGTTTTACAGGTGGCGCACTGGACAA
AGCAAAATTTGATACCTATCCGCTGGCAGGTAGCCCGAAAAAACCGC
TGAAACTGAAGGGTCGCTTTTTGGATTA AAAAGGGTTTTAGCGGTGAT
CACAAAGCTGCTGATTACCACAGCACTGAGCGATATTCGTGATGGCCT
GTATCCTCTGGGTAGTAAAGGTGGTGTGGTTATGGTTGGGTTGCAGG
TATTAGCATTGATGATAATGTGCCGGATGACTTTAAAGAGATGATCA
ACAAGACAGAAATGCCGCTGCCGGAAGAAGTGGAAGAAAGCAATAA
TGGTCCGATCAATAACGATTATGTTTCATCCGGGTCATCAGAGCCCGA
AACAGGATCATAAAAACAAGAACATCTATTATCCGCATTATTTTCTGG
ACAGCGGCAGCAAAGTGTATCGCGAAAAAGATATTATCACCCACGAA
GAATTCACCGAGGAACTGCTGTCAGGCAAAATTA ACTGTAAACTTGA
AACCTTGACACCGCTGATTATTCGGATACCAGTGATGAAAATGGTC
TGAAACTTCAGGGTAATAAACCGGGTCATAAGAACTACAAATTCCTC
AACATTAATGGCGAACTGATGATTCCGGGTT CAGA ACTGCGTGGCAT
GCTGCGCACCCATTTTGAAGCACTGACCAAAAGCTGTTTTGCCATTTT
TGGTGAAGATAGCACCCCTGAGCTGGCGTATGAATGCAGATGAGAAAG
ATTACAAAATCGATAGCAACAGCATCCGCAAAATGGAAAGCCAGCGT
AATCCGAAATATCGCATTCCGGACGAACTGCAGAAAGAGCTGCGTAA
TAGCGGTAATGGTCTGTTTAATCGTCTGTATAACCAGCGAACGTCGTTT
TTGGAGTGATGTGAGTAACAAATTTGAGAACAGCATCGATTACAAC
GCGAAATTCTGCGTTGTGCAGGTCGTCCGAAAAACTATAAAGGCGGT
ATTATTCGTCAGCGTAAAGATAGTCTGATGGCCGAAGAACTGAAAGT
TCATCGTCTGCCTCTGTATGATAACTTTGATATTCCTGATAGCGCCTA
CAAAGCCAACGATCATTGTCTGTA AAAAGCGCAACCTGTAGCACCAGCC
GTGGTTGTCGTGAACGTTTTACCTGTGGCATTAAAGTGCGTGATAAAA
ATCGCGTTTTTTCTGAATGCAGCCAATAATAATCGCCAGTACCTGAACA
ACATCAAAAAGTCCAATCACGATCTGTATCTGCAGTATCTGAAAGGC
GAAAAAAAGATCCGCTTCAACAGCAAAGTTATTACAGGTAGCGAACG
TAGCCCGATTGATGTTATTGCAGA ACTGAATGAACGTGGTTCGTCAGA
CCGGTTTTATCAA ACTGAGCGGTCTGAATAACAGCAATAAAAAGCCAG
GGCAATACCGGCACCACATTTAATAGTGGTTGGGATCGCTTTGAACT
GAATATACTGCTGGATGATCTGGAAACCCGTCCGAGCAAAAGCGATT
ATCCGCGTCCGCGTCTGCTGTTTACCAAAGATCAGTATGAATACAACA
TCACCAAACGTTGCGAACGCGTGTGTTT GAAATTGATAAAGGCAACAAA
ACAGGCTATCCGGTGGATGATCAGATCAAAAAGAACTACGAAGATAT
CCTGGACAGCTATGATGGCATCAAAGATCAAGAAGTTGCCGAACGCT
TTGATACATTTACCCGTGGTAGCAAGCTGAAAGTTGGCGATCTGGTTT
ATTTTCATATCGACGGCGATAACAAAATTGACAGCCTGATTCCGGTTC
GTATTAGCCGTAAATGTGCAAGCAAAACCTTAGGTGGCAAATTAGAT
AAAGCACTGCATCCGTGCACCGGTCTGTCAGATGGTCTGTGTCCGGGT

	<p>TGTCACCTGTTTGGCACCACCGATTATAAAGGTTCGCGTTAAATTTGGC TTCGCCAAATATGAAAACGGTCCTGAATGGCTGATTACGCGTGGTAA TAATCCGGAACGTAGTCTGACCCTGGGTGTGCTGGAATCACCGCGTC CGGCATTTTCAATTCCGGATGATGAAAGTGAAATTCCGGGTCGTA TTCTATCTGCATCACAATGGTTGGCGCATTATTCGCCAGAAACA ACTGAAATTCGTGAAACCGTTCAGCCGGAACGCAATGTTACCACCGAAGT GATGGATAAAGGTAACGTGTTTAGCTTTGATGTGCGCTTTGAAAATCT GCGTGAATGGGAACCTGGGTCTGCTGCTGCAGAGTCTGGATCCTGGTA AAAACATTGCACATAAACTTGGTAAAGGCAAACCGTATGGTTTTGGC AGCGTGAAAATCAAGATTGATAGCCTGCATACCTTCAAGATTAACAG CAACAACGACAAAATCAAACGTGTTCCGCAGAGTGATATCCGCGAGT ATATTAACAAAGGCTACCAGAACTGATTGAATGGTCAGGTAATAAT AGCATCCAGAAAGGTAATGTGCTGCCGCAAGTGGCATGTTATTCCGCA TATTGACAACTGTACAACTGCTGTGGGTTCGTTTCTGAACGATAG CAAACCTGGAACCGGATGTTTCGTTATCCGGTCTGAATGAAGAATCCA AAGGTTATATTGAGGGCAGCGATTACACCTATAAAAAGCTGGGAGAT AAAGATAACCTGCCGTATAAAACCCGTGTTAAAGGTCTGACCACACC GTGGTCACCGTGGAATCCGTTTCAGGTGATTGCCGAACATGAAGAAC AAGAAGTGAACGTTACCGGTAGCCGTCCGAGTGTTACCGATAAAATT GAACGTGATGGTAAAATGGTGTA</p>
CRISPR-1 array	<p>ATATATCATATGTACAAAATGGCCCCTTCTCGCCATATACGTAACCTC AGAGTTGTTGGAGGGTTATGAAACAAGAGAAGGACTTAATGTCACGG TACCCAATTTTCTGCCCGGACTCCACGGCTGTTACTAGAGGTTATGA AACAAAGAGAAGGACTTAATGTCACGGTACCCAATTTTCTGCCCGGA CTCCACGGCTGTTACTAGAGGTTATGAAACAAGAGAAGGACTTAATG TCACGGTACCCAATTTTCTGCCCGGACTCCACGGCTGTTACTAGAGG TTATGAAACAAGAGAAGGACTTAATGTCACGGTACCCAATTTTCTGC CCCGGACTCCACGGCTGTTACTAGAGGTTATGAAACAAGAGAAGGAC TTAATGTCACGGTACCCAATTTTCTGCCCGGACTCCACGGCTGTTAC TAGAGGTTATGAAACAAGAGAAGGACTTAATGTCACGGTACCAATTG ATATAT</p>
CRISPR-3 array	<p>ATATATCATATGTACAAAATGGCCCCTTCTCGCCATATACGTAACCTC AGAGTTGTTGGAGGGTTATGAAACAAGAGAAGGACTTAATGTCACGG TACAATTATCATTTGGACAGCTTCCCTCATTATTTTCGAGGTCGTTATG AAACAAGAGAAGGACTTAATGTCACGGTACAATTATCATTTGGACAG CTTCCCTCATTATTTTCGAGGTCGTTATGAAACAAGAGAAGGACTTAAT GTCACGGTACAATTATCATTTGGACAGCTTCCCTCATTATTTTCGAGG CGTTATGAAACAAGAGAAGGACTTAATGTCACGGTACAATTATCATT TGGACAGCTTCCCTCATTATTTTCGAGGTCGTTATGAAACAAGAGAAG GACTTAATGTCACGGTACAATTATCATTGGACAGCTTCCCTCATTAT TTCGAGGTCGTTATGAAACAAGAGAAGGACTTAATGTCACGGTACCA ATTGATATAT</p>
Codon-optimized	<p>ATTGTGAGCGGATAACAATTCCCCTGTAGAAATAATTTGTTTAACTT TAATAAGGAGATATACCATGAACAACACCGAAGAAAACATCGATCGT</p>

TPR-CHAT
(C-terminal
His-tag)

ATTCAAGAACCGACGCGTGAAGATATTGATCGTAAAGAAGCAGAACG
TCTGCTGGATGAAGCATTTAATCCGCGTACCAAACCGGTGGATCGCA
AAAAAATCATTAAATAGCGCACTGAAAATTCTGATCGGCCTGTACAAA
GAGAAAAAAGACGATCTGACCAGCGCAAGCTTTATTAGCATTGCACG
TGCCTATTATCTGGTGAAGCATTACCATTCTGCCGAAAGGCACCACCAT
TCCGGAAAAAAGAAAGAAGCACTGCGCAAAGGCATCGAATTTATTG
ATCGCGCAATCAACAAGTTTAACGGCAGCATTCTGGATAGCCAGCGT
GCATTTTCGTATTAAGAGCGTTCTGAGCATTGAGTTCAATCGTATCGAT
CGTGAAAAATGCGACAACATCAAACCTGAAAAACCTGCTGAACGAAG
CCGTTGATAAAGGTTGTACCGATTTTGATACCTATGAGTGGGATATTC
AGATTGCCATTCGTCTGTGTGAACTGGGTGTTGATATGGAAGGTCATT
TTGACAACCTGATCAAAAGCAACAAAGCCAACGATCTGCAGAAAGCC
AAAGCCTATTACTTCATCAAAAAGGATGACCATAAAGGCCAAAGAACA
CATGGATAAATGTACCGCAAGCCTGAAATATAACCCCGTGTAGTCATC
GTCTGTGGGATGAAACCGTTGGTTTTATTGAACGTCTGAAAGGTGATA
GCAGCACCTGTGGCGTGATTTTGAATTAACCTATCGTAGCTGCC
GTGTGCAAGAAAAAGAAACCGGTACACTGCGTCTGCGTTGGTATTGG
AGCCGTCATCGTGTCTGTATGATATGGCATTCTGGCAGTTAAAGAA
CAGGCAGATGATGAAGAACCGGATGTTAATGTTAAACAGGCCAAAAT
CAAAAAGCTGGCCGAAATTAGCGATAGCCTGAAAAGCCGTTTTAGCC
TGCCTCTGAGCGATATGGAAAAAATGCCGAAAAGTGATGATGAAAGC
AACCACGAGTTCAAAAAGTTTCTGGACAAATGTGTTACCGCCTATCA
GGATGGTTATGTGATTAATCGTAGCGAGGATAAAGAAGGTCAGGGCG
AAAACAAAAGCACCACCAGTAAACAGCCGGAACCGCGTCCGCAGGC
AAAACCTGCTGGAACCTGACCCAGGTTCCGGAAGGTTGGGTTGTTGTT
ACTTTTATCTGAATAAACTGGAAGGTATGGGCAACGCCATTGTGTTTG
ATAAATGTGCAAATAGCTGGCAGTACAAAGAATTTTCAGTATAAAGAA
CTGTTTGAAGTGTTCTGACCTGGCAGGCAAACCTATAATCTTTACAAA
GAAAACGCAGCCGAACATCTGGTTACCCTGTGTAAAAAGATTGGTGA
AACCATGCCGTTTCTGTTCTGCGATAACTTTATTCCGAATGGTAAAGA
TGTTCTGTTTGTGCCGCATGATTTTCTGCATCGTCTGCCGCTGCATGGT
AGCATTGAGAATAAAACAAATGGCAAGCTGTTCTGGAATAATCATAG
CTGTTGTTATCTGCCTGCATGGTCATTTGCAAGCGAAAAAGAAGCAA
GCACCAGCGACGAATATGTTCTGCTGAAAAATTTTCGATCAGGGCCAT
TTTGAAACCCTGCAGAATAATCAGATTTGGGGCACCCAGAGCGTTAA
AGATGGTGCAAGCAGTGATGATCTGGAAAACATTCGTAACAATCCGC
GTCTGCTGACCATTCTGTGTCATGGTGAAGCAAATATGAGCAATCCGT
TTCGTAGCATGCTGAAACTGGCAAATGGTGGTATTACCTATCTGGAA
ATTCTGAATAGCGTGAAAGGCCTGAAAGGTAGCCAGGTTATTCTGGG
TGCATGTGAAACCGATCTGGTTCCGCCTCTGAGTGATGTTATGGATGA
ACATTATAGCGTTGCAACCGCACTGCTGCTGATTGGTGCAGCGGGTGT
TGTTGGCACCATGTGGAAAGTTCGTAGCAATAAAACGAAAAGCCTGA
TCGAGTGGAAGCTGGAAAATATCGAATATAAACTGAACGAGTGGCAG
AAAGAAACAGGTGGTGCAGCATATAAAGATCATCCGCCTACCTTTTA
TCGTAGCATTGCCTTTTCGTAGTATTGGTTTTCCGTTAGGTGGTAGCGG
TCATCACCATCACCACCATCATTAATCTACTAGCGCAGCTTAATT
AACCTAGGCTGCTGCCACCGCTGAGCAATAACTAGC

Codon- optimized TPR-CHAT H585A C627A insertion	AATCCGCGTCTGCTGACCATTCTGTGTGCGGGTGAAGCAAATATGAG CAATCCGTTTCGTAGCATGCTGAAACTGGCAAATGGTGGTATTACCTA TCTGGAAATTCTGAATAGCGTGAAAGGCCTGAAAGGTAGCCAGGTTA TTCTGGGTGCAGCGGAAACCGATCTGGTTCCGCCTCTGAGTGAT
----------------------------------------------------------------	--------------------------------------------------------------------------------------------------------------------------------------------------------------------------------------------------------